

Triggers for displaced decays of long-lived neutral particles in the ATLAS detector

This article has been downloaded from IOPscience. Please scroll down to see the full text article.

2013 JINST 8 P07015

(<http://iopscience.iop.org/1748-0221/8/07/P07015>)

View [the table of contents for this issue](#), or go to the [journal homepage](#) for more

Download details:

IP Address: 137.138.125.164

The article was downloaded on 16/09/2013 at 14:05

Please note that [terms and conditions apply](#).

Triggers for displaced decays of long-lived neutral particles in the ATLAS detector



The ATLAS collaboration

E-mail: atlas.publications@cern.ch

ABSTRACT: A set of three dedicated triggers designed to detect long-lived neutral particles decaying throughout the ATLAS detector to a pair of hadronic jets is described. The efficiencies of the triggers for selecting displaced decays as a function of the decay position are presented for simulated events. The effect of pile-up interactions on the trigger efficiencies and the dependence of the trigger rate on instantaneous luminosity during the 2012 data-taking period at the LHC are discussed.

KEYWORDS: Trigger concepts and systems (hardware and software); Online farms and online filtering; Trigger algorithms

Contents

1	Introduction	1
2	The ATLAS detector	2
3	Benchmark model and decay signature	3
4	Decays in the inner detector and electromagnetic calorimeter	5
5	Decays in the hadronic calorimeter	6
6	Decays in the muon spectrometer	9
7	Trigger efficiency on simulated events	13
8	Triggering on collision data	16
9	Conclusions	17
	The ATLAS collaboration	20

1 Introduction

Many extensions to the Standard Model (SM) include the production of neutral, weakly-coupled and long-lived particles that can decay to final states containing several hadronic jets. These long-lived particles occur in many models such as Gauge Mediated Supersymmetry Breaking (GSMB) [1], the Minimal Supersymmetric Standard Model (MSSM) with R-parity violation [2], inelastic dark matter [3] and Hidden Valley (HV) scenarios [4–6]. Such neutral particles with a potentially long decay path present a trigger and reconstruction challenge for the LHC detectors in that they have no detector activity connecting them to the primary interaction point (IP). Depending on the kinematics of the production mechanism and the masses of the parent and long-lived objects, these events may be displaced in time from the events selected by the standard triggers. In this paper we discuss the signature-driven triggers developed by the ATLAS Collaboration to select these events. To evaluate these triggers we use as a benchmark an HV scenario, in which the SM is weakly coupled, by a heavy communicator particle, to a hidden sector that includes a neutral pseudoscalar pion, π_ν . The π_ν can have a long lifetime resulting in decays far from the IP. One of these triggers was successfully used for the recently published search for a light Higgs boson decaying to long-lived neutral particles [7].

Section 2 describes the ATLAS detector and trigger system, section 3 discusses the benchmark model and the decay signatures, sections 4–6 describe the long-lived neutral particle triggers, section 7 presents trigger performance on simulated events and section 8 discusses trigger performance in the 2012 data-taking period.

2 The ATLAS detector

ATLAS is a multi-purpose detector [8] consisting of an inner tracking system (ID) embedded in a superconducting solenoid, electromagnetic (ECal) and hadronic (HCal) calorimeters and a muon spectrometer (MS) with three air-core toroidal magnetic fields. The ID consists of a silicon pixel detector, a silicon strip detector (semiconductor tracker, SCT) and a straw tube tracker (transition radiation tracker, TRT) and provides precision tracking of charged particles for $|\eta| \leq 2.5$.¹ The ID extends from a radius, r , of 0.05 m to 1.1 m and in $|z|$ to 3.5 m. The ECal and HCal systems cover the region $|\eta| \leq 4.9$ and have a thickness of 9.7 interaction lengths at $\eta = 0$. In the region $|\eta| \leq 3.2$ electromagnetic calorimetry is provided by barrel and end-cap high-granularity lead/liquid-argon (lead/LAr) electromagnetic calorimeters. An additional thin LAr presampler covering $|\eta| \leq 1.8$ is used to correct for energy loss in the material upstream of the calorimeters. Hadronic calorimetry is provided by a steel/scintillator tile calorimeter that is segmented into three barrel structures for $|\eta| \leq 1.7$ and two copper/LAr hadronic end-cap calorimeters that extend the coverage to $|\eta| \leq 3.2$. The solid angle coverage is completed up to $|\eta| \leq 4.9$ with forward calorimeter modules optimized for both electromagnetic and hadronic measurements. The ECal extends from r of 1.5 m to 2.0 m in the barrel and from $|z|$ of 3.6 m to 4.25 m in the end-caps. The HCal covers the region r from 2.25 m to 4.25 m in the barrel and $|z|$ from 4.3 m to 6.05 m in the end-caps. The MS provides trigger and momentum measurements for charged particles entering the spectrometer. It consists of one barrel and two end-caps, each with 16 sectors, equipped with fast detectors for triggering and precision tracking chambers, monitored drift tubes (MDT) and cathode strip chambers (CSC). In the MS barrel region, tracks are measured in chambers arranged in three cylindrical layers around the beam axis; in the transition and end-cap regions, the chambers are installed in planes perpendicular to the beam, also in three layers. An air-core toroidal field allows accurate charged particle reconstruction independent of the ID information. For triggering, three stations of resistive plate chambers (RPC) and thin gap chambers (TGC) are used in the MS barrel and end-caps, respectively. The first two RPC stations are located at a radius of 7 m (large sectors²) and 8 m (small sectors) with a separation of 0.5 m; the third station is at a radius of 9 m (large sectors) and 10 m (small sectors). In the end-caps the first TGC station is located at $|z| = 13$ m and the other two at 14 m with a separation of 0.5 m.

The trigger system has three levels [9]. The first level (L1) is a hardware-based system using information from the calorimeter and the muon detectors. The second (L2) and third (Event Filter, EF) levels are software-based systems using information from all of the ATLAS detectors. Together, L2 and EF are called the High Level Trigger (HLT). The L1 trigger uses information based on relatively coarse data from the calorimeters and the muon trigger stations. The L1 thresholds are applied to transverse energy (E_T) for calorimeter-based triggers and transverse momentum (p_T) for muon triggers. The L1 trigger identifies Regions of Interest (RoIs), which are (η, ϕ) regions of the detector associated to a specific physics signature. RoIs are widely used in the subsequent

¹The ATLAS reference system is a cartesian right-handed coordinate system, with the nominal collision point at the origin. The anti-clockwise beam direction defines the positive z -axis, with the x -axis pointing to the centre of the LHC ring. The angle ϕ defines the direction in the plane (x, y) transverse to the beam. The pseudorapidity is given by $\eta = -\ln \tan(\theta/2)$, where the polar angle θ is taken with respect to the positive z direction.

²The barrel chamber system is subdivided into large (between the magnet coils) and small (inside the magnet coils) sectors.

Table 1. Mass and mean proper lifetime parameters for the simulated benchmark models.

Higgs boson mass [GeV]	π_v mass [GeV]	π_v mean proper lifetime [m]
100	25	0.125
126	10	0.35
140	20	0.63

trigger levels to reduce the amount of data read from the detector readout buffers while accessing the full information for the most important part of the event.

The L1 muon trigger logic is implemented in similar ways for both the RPC and TGC systems. Each of the three planes of the RPC system and the two outermost planes of the TGC system consist of a doublet of independent detector layers while the first TGC plane contains three detector layers. A low- p_T muon RoI is generated by requiring a coincidence of hits in at least three of the four layers of the two inner RPC planes for the barrel and of the two outer TGC planes for the end-caps. A high- p_T muon RoI requires additional hits in at least one of the two layers of the outer RPC plane for the barrel and in two of the three layers of the innermost TGC layer for the end-caps. The muon RoIs have a spatial extent of 0.2 in $\Delta\eta$ and $\Delta\phi$ in the MS barrel and 0.1 in the MS end-caps. Only the two highest- p_T RoIs per MS sector are used by the HLT.

The L1 calorimeter trigger provides the capability to search for trigger objects such as electrons, photons, τ leptons, jets and transverse energy based on information from the calorimeter elements within projective regions, called trigger towers. The trigger towers have a size of approximately 0.1 in $\Delta\eta$ and $\Delta\phi$ in the central part of the calorimeter, $|\eta| < 2.5$, and are larger and less uniform in the more forward region.

3 Benchmark model and decay signature

An HV model with a light Higgs mediator is used to evaluate the ATLAS detector response to highly displaced decays to hadronic jets. Three different Monte Carlo (MC) simulation samples are used for this study. In each sample, a Higgs boson is produced via gluon fusion and decays to a pair of long-lived π_v particles. Because the π_v is a pseudoscalar, it decays predominantly to heavy fermions, $b\bar{b}$, $c\bar{c}$ and $\tau^+\tau^-$ in the ratio 85:5:8, as a result of the helicity suppression of the low-mass fermion anti-fermion pairs.³

The parameters used to generate the samples are summarized in table 1. The mean proper lifetime values are chosen to maximize the number of simulated π_v decays for all of the ATLAS detectors. The masses are chosen to give a range of β (speed relative to the speed of light in vacuum) distributions of the π_v particles in order to study trigger timing and correct bunch crossing identification. The events are generated at a center-of-mass energy of 8 TeV using Pythia 8.165 [10]. The MSTW 2008 leading order parameterization [11] is used for the parton distribution functions in the proton. The mean value of $\langle\mu\rangle$ used in the simulation is 22 and the distribution follows the predicted conditions for the 2012 $\sqrt{s} = 8$ TeV data, which ranged in instantaneous luminosity

³Hidden sector scalars that couple to the SM via their mixings with the Higgs boson have Yukawa interactions with fermions and anti-fermions and these couplings are proportional to the fermion masses; therefore, these scalars decay in a similar way to the pseudoscalar π_v particles.

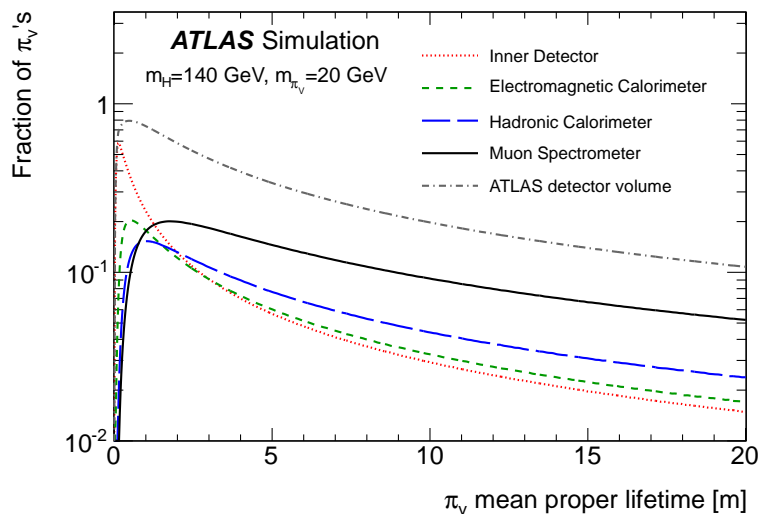


Figure 1. The probability of a π_0 to decay in the ID (beyond the second layer of the pixel detector), ECal, HCal, MS and the whole ATLAS detector as a function of the π_0 mean proper lifetime ($c\tau$) for $|\eta| < 2.5$. The sample with $m_H = 140$ GeV and $m_{\pi_0} = 20$ GeV is used.

from approximately 2 to $7 \times 10^{33} \text{ cm}^{-2} \text{ s}^{-1}$. The quantity μ is a measure of the average number of inelastic interactions per bunch crossing and $\langle \mu \rangle$, the average value over all proton bunches, gives the average number of expected proton-proton collisions per event.

Figure 1 shows the probability for a π_0 to decay in the barrel and end-caps fiducial regions of the ATLAS detector as a function of the π_0 mean proper lifetime. There is a substantial probability (greater than 10%) for decays to occur in the ATLAS detector volume for a wide range of mean proper lifetimes. For example, with a mean proper lifetime of 2 m the total fraction of π_0 decays in the ATLAS detector is 58%, of which 13% are in the ID, 12% are in the ECal, 13% are in the HCal and 20% are in the MS.

With the exception of the novel triggers described in this paper, the ATLAS triggers were designed to select physics objects originating at (or near) the IP. Events with long-lived particles present many challenges for the trigger system: for example, muons from π_0 decays do not have associated tracks in the ID, while jets from π_0 decays may have relatively low energy, not have the usual pattern of energy deposition and arrive later than expected. Typical signatures of π_0 decays to hadronic jets occurring in the ID, HCal and MS are shown in figures 2(a) and 2(b).

In order to improve the trigger efficiency, a set of signature-driven triggers were developed to select events based on the detector signature of the displaced hadronic jets. Three regions of the detector are considered: decays beyond the pixel layers to the ECal, decays in the HCal and decays from the end of the HCal to the MS middle station. For each of these regions a unique decay signature exists that can be exploited to select events with displaced decays in the region $|\eta| < 2.5$ for which tracking information is available.

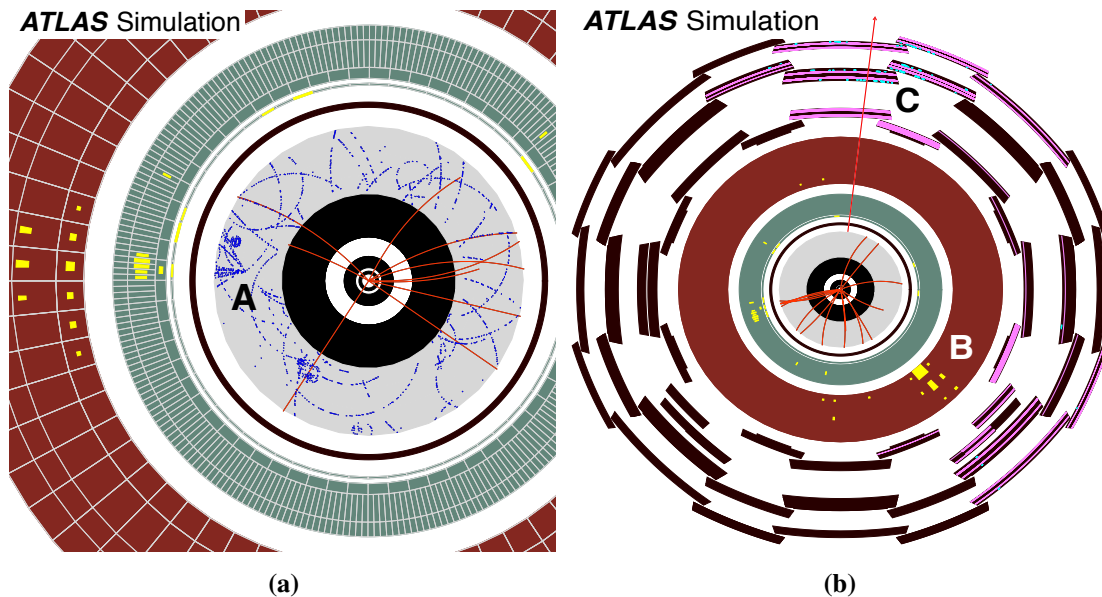


Figure 2. Event displays of two simulated $H \rightarrow \pi_\nu \pi_\nu$ events with different π_ν decay signatures to hadronic jets. The sample with $m_H = 140$ GeV and $m_{\pi_\nu} = 20$ GeV is used. The ATLAS detectors are depicted in different colours: black for the pixel detector and the SCT, light gray for the TRT, green for the ECal, red for the HCal and again black for the MS. The solenoid and the pre-sampler calorimeter are shown as the black and green rings between the ID and the ECal. (a) Event display with one π_ν decay in the ID (A). The display focuses on the innermost part of the ATLAS detector. TRT hits clearly indicate the presence of a displaced decay on the left side of the detector, matching well with the energy deposited in the ECal. (b) Event display with one π_ν decay in the HCal (B) with the signature of little activity in the ID and a jet with all of the energy deposit in the HCal and a second decay in the MS (C). The RPC hits are displayed as sky-blue dots and the MDT hits as pink lines. The red arrow indicates the direction of the missing transverse momentum that correctly points towards the π_ν decay in the MS.

4 Decays in the inner detector and electromagnetic calorimeter

A decay topology with two jets characterizes most of the events where both π_ν decays are in the ECal volume, as shown in figure 3(a). Decays that occur beyond the pixel detector produce jets that have no tracks reconstructed by the L2 track reconstruction algorithm. This results in a characteristic signature of a jet isolated with respect to tracks in the ID. A large fraction of jets originating from π_ν decays beyond the pixel detector have no reconstructed tracks with $p_T > 0.8$ GeV in a region of (0.2×0.2) in $(\Delta\eta \times \Delta\phi)$ centred on the jet axis, as can be seen in figure 3(b). A jet fulfilling these requirements is defined as a “trackless jet”.

The trackless jet signature provides a powerful handle for identifying jets from displaced decays. Because tracking is not available until the HLT, a different approach is necessary to get a sustainable L1 output rate while not compromising the signal efficiency. In signal events there is a $\sim 40\%$ probability to produce a muon in the final state. Thus, the multi-jet background can be

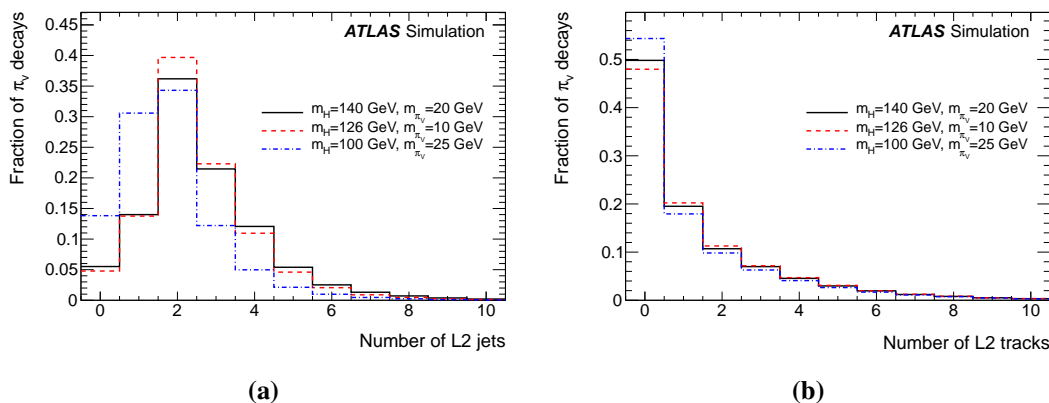


Figure 3. (a) Number of reconstructed jets at L2 with $E_T > 25$ GeV and $|\eta| < 2.5$ in events where both π_ν decays are beyond the pixel detector and before the HCal volume. (b) Number of reconstructed tracks in the ID at L2 with $p_T > 0.8$ GeV in a (0.2×0.2) region in $(\Delta\eta \times \Delta\phi)$ around the jet axis of a L2 jet with $E_T > 25$ GeV and $|\eta| < 2.5$ in events where both π_ν decays are beyond the pixel detector and before the HCal volume.

significantly reduced by requiring the muon to be contained within the jet cone. In multi-jet events produced via SM processes, the muon will typically be prompt and thus leave a track in the ID, while in π_ν events the muon is produced close to the π_ν decay vertex and can be highly displaced from the IP. Requiring both a jet trigger item and a muon trigger item at L1 is therefore a good handle for limiting the L1 output rate. The two objects are required to be in the same detector region at L2 and to be isolated with respect to tracks reconstructed in the ID.

The Trackless Jet trigger implementation requires a muon with $p_T > 10$ GeV and a jet with $E_T > 20$ GeV at L1. The L2 jet and muon reconstruction algorithms are then employed in the corresponding RoIs to confirm and refine the physics objects identified at L1. Because the particles from displaced decays do not have reconstructable tracks in the ID, the L2 muon reconstruction algorithm is restricted to run only in the MS. The criteria at L2 are $p_T > 10$ GeV for the muon and $E_T > 25$ GeV for the jet, where the calorimeter response is calibrated at the electromagnetic (EM) scale, which is tuned to correctly measure the energy of EM showers. A combinatorial algorithm performs a geometrical matching in a $\Delta R \equiv \sqrt{(\Delta\eta)^2 + (\Delta\phi)^2} = 0.4$ region between the muon and jet objects. The final criterion of no tracks in the ID with $p_T > 0.8$ GeV in a (0.2×0.2) region in $(\Delta\eta \times \Delta\phi)$ around the jet direction is made at L2. No further selection is applied at the EF. A schematic diagram of the sequence of algorithms employed in the Trackless Jet trigger is depicted in figure 4(a).

5 Decays in the hadronic calorimeter

Decays of neutral particles in the outer layers of the ECal or in the HCal result in little or no energy deposited in the ECal (figure 2) and consequently in an anomalously large value of the hadronic to electromagnetic energy ratio, E_{HAD}/E_{EM} , of the jet. Since the neutral π_ν has travelled through the tracking volume without interacting before decaying in the calorimeter, no reconstructed tracks connecting the jet to the primary IP are expected. Another feature of this topology is that the pair

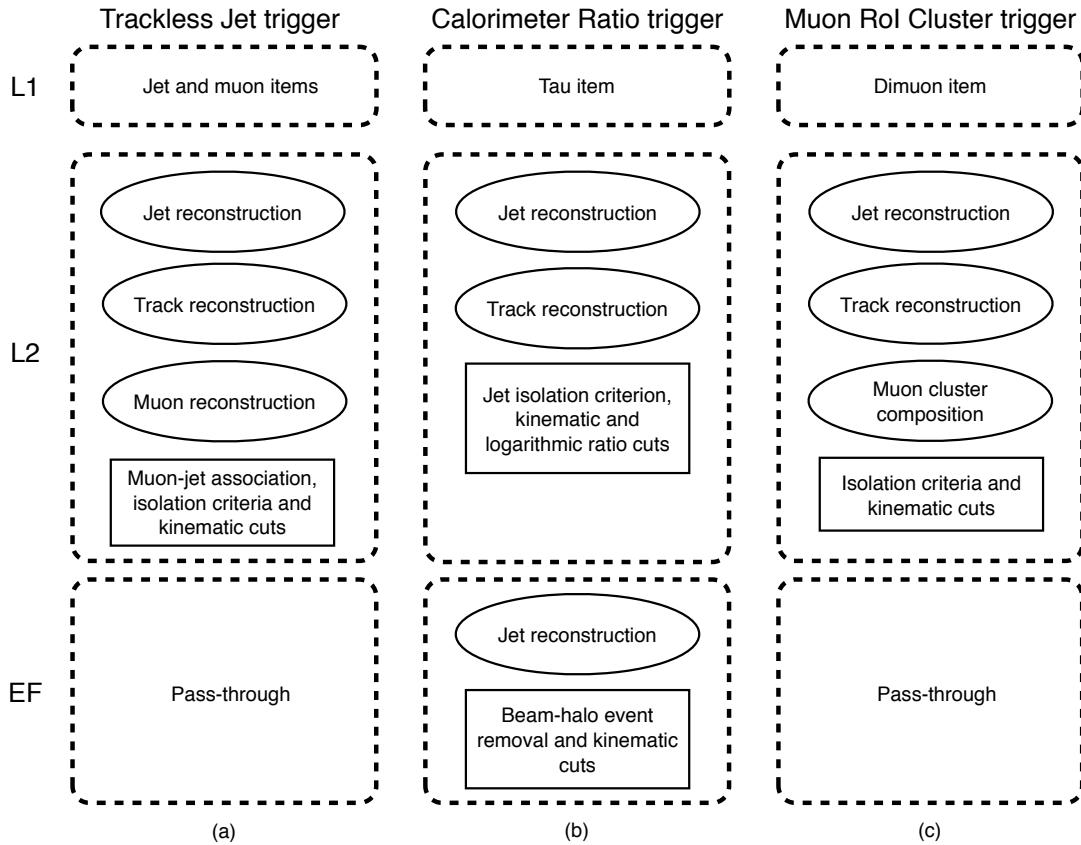


Figure 4. Schematic diagrams of the sequence of trigger algorithms used to select long-lived neutral particles decaying throughout the ATLAS detector volume: Trackless Jet trigger (a), Calorimeter Ratio trigger (b) and Muon RoI Cluster trigger (c). The ovals represent trigger algorithms to reconstruct features while rectangles represent trigger algorithms that apply cuts using the reconstructed features.

of hadronic jets doesn't have time to spatially separate before depositing its energy in the HCal and this results in a very narrow single jet being reconstructed. The ‘‘Calorimeter Ratio trigger’’ is designed to select this signature.

As can be seen in figure 5(a), almost all of the energy from jets originating from π_ν decays in the HCal is contained within a cone of $\Delta R = 0.1$ around the jet axis. For this reason, a L1 τ -lepton trigger is preferable to a L1 jet trigger because the latter selects events in a $(\Delta\eta \times \Delta\phi)$ region of (0.4×0.4) while the former selects, by design, jets with energy contained in a region of (0.2×0.2) , which better matches the narrow jets produced when a π_ν decays in the HCal. The τ -lepton triggers also have a lower energy threshold than the jet triggers, resulting in an increase of the signal efficiency relative to the multi-jet background acceptance. Figure 5(b) shows the mean value of the $\log_{10}(E_{\text{HAD}}/E_{\text{EM}})$ distribution for all L2 jets from π_ν decays in the barrel calorimeter as a function of the π_ν radial decay distance. As the π_ν decays close to the end of the ECal, the logarithmic ratio changes from a characteristic negative value to a positive value. The average value of $\log_{10}(E_{\text{HAD}}/E_{\text{EM}})$ plateaus at ~ 1.5 for radii between ~ 1.9 m and ~ 3.6 m, at which point the π_ν decay occurs too close to the outer radius of the HCal to reconstruct a jet. The Gaussian width (σ) of

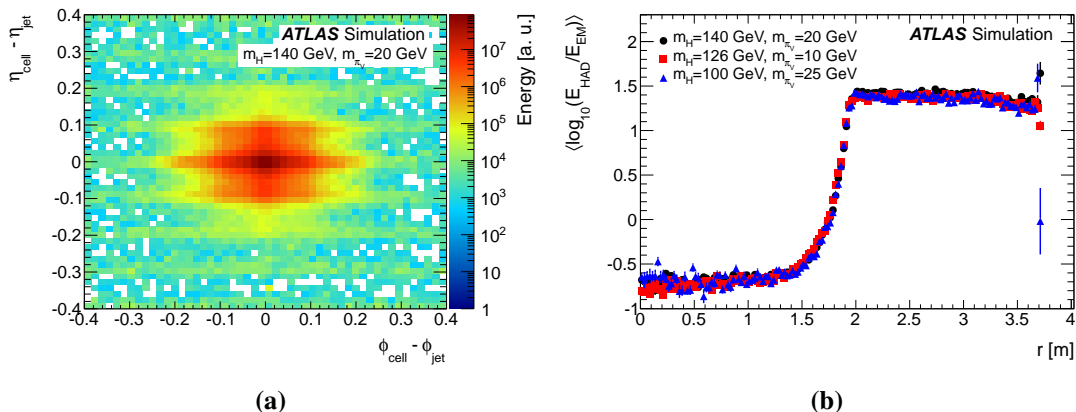


Figure 5. (a) Energy deposition in the calorimeter cells around the jet axis (0,0) for π_ν decays in the HCal. (b) Mean value of $\log_{10}(E_{\text{HAD}}/E_{\text{EM}})$ for all L2 jets in the barrel calorimeter coming from π_ν decays as a function of the π_ν radial decay distance, r .

the $\log_{10}(E_{\text{HAD}}/E_{\text{EM}})$ distribution beyond 2 m is 0.35. Because jets with $\log_{10}(E_{\text{HAD}}/E_{\text{EM}}) > 1.2$ are produced by π_ν decays in the calorimeter, the ID should not contain any tracks pointing to a signal jet. The result of applying the L2 tracking algorithm is that about 80% of the jets with $\log_{10}(E_{\text{HAD}}/E_{\text{EM}}) > 1.2$ have no tracks with $p_T > 1$ GeV reconstructed in a region of (0.2×0.2) in $(\Delta\eta \times \Delta\phi)$ around the jet axis, as shown in figure 6(a).

The π_ν particles from Higgs decay have $\beta < 1$ and arrive in the calorimeter later than a $\beta = 1$ particle. The signal peak amplitude is thus shifted later in time, and this affects the raw energy measurement. The online Optimal Filtering Algorithm [12] determines this time shift and provides a corrected energy at L2 that is within 1% of the true energy for time shifts of up to 12 ns [13]. Figure 6(b) from the ATLAS simulation of the calorimeter trigger, which incorporates the Optimal Filtering Algorithm and energy correction algorithms, shows that for the m_H and m_{π_ν} combinations considered, more than 93% of the π_ν decays in the HCal have a time shift of less than 10 ns for a broad range of mean proper lifetimes.

Beam-halo muons that undergo bremsstrahlung as they traverse the HCal are a potential source of background for the Calorimeter Ratio trigger. If an energetic bremsstrahlung radiation is emitted by the muon in the HCal, the L1 trigger logic interprets this energy deposit as a jet and the event is passed to L2; no energy is found in the ECal and therefore the event is accepted at L2. In order to discard these events, an additional algorithm, exploiting the non-collision-like timing signature in the HCal, is implemented in the EF of the Calorimeter Ratio trigger. If at least three HCal cells with $E > 240$ MeV are found with a difference in timing of 5 ns with respect to a particle travelling at $\beta = 1$, the event is rejected. Only cells within $|\Delta\phi| < 0.2$ and $\Delta R > 0.3$ from the leading jet axis are considered. The removal of beam-halo muons reduces the Calorimeter Ratio trigger rate by almost 50% without compromising the signal acceptance.

The Calorimeter Ratio trigger is built by requiring a τ -lepton object with $E_T > 40$ GeV at L1. The threshold at 40 GeV corresponds to the lowest unprescaled L1 τ -lepton item used during data taking in 2012. The L2 jet and track reconstruction algorithms are then employed using the L1 τ -lepton RoI as input. The L2 reconstructed jet is required to have $E_T > 30$ GeV, with the calorimeter

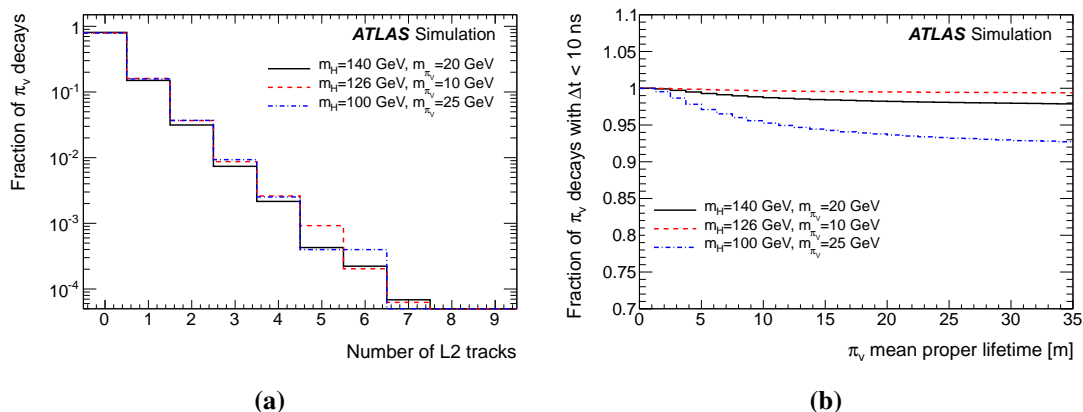


Figure 6. (a) Distribution of the number of reconstructed tracks in the ID at L2 with $p_T > 1$ GeV in a (0.2×0.2) region in $(\Delta\eta \times \Delta\phi)$ around the jet axis of a L2 jet with $\log_{10}(E_{\text{HAD}}/E_{\text{EM}}) > 1.2$ and $|\eta| < 1.5$ in events where the π_ν decays in the HCal. (b) Fraction of π_ν decays in the HCal with a delay of $\Delta t < 10$ ns as a function of the π_ν mean proper lifetime.

response calibrated at the EM scale. Two additional criteria are applied: that there be no tracks with $p_T > 1$ GeV reconstructed in a (0.2×0.2) region in $(\Delta\eta \times \Delta\phi)$ around the jet direction and that the jet $\log_{10}(E_{\text{HAD}}/E_{\text{EM}}) > 1.2$. At the EF, the standard anti- k_t jet-finding algorithm [14] is added to refine the jet object properties and $E_T > 35$ GeV is required. The final criterion removes beam-halo events. A schematic diagram of the sequence of algorithms employed in the Calorimeter Ratio trigger is depicted in figure 4(b).

6 Decays in the muon spectrometer

Decays occurring at the outermost regions of the HCal or in the MS result in a large number of charged hadrons traversing a narrow region of the MS. These events are characterized by a cluster of L1 muon RoIs centred around the π_ν line of flight.

Figures 7(a) and 7(b) show the total number of muon RoIs found in events with a π_ν decaying in the MS barrel or end-caps. Larger ROI multiplicities are found in the end-caps because the muon RoIs have a spatial extent of 0.1 in $\Delta\eta$ and $\Delta\phi$ in the end-caps compared to 0.2 in the barrel. Figures 8(a) and 8(b) show the average number of L1 muon RoIs contained in a cone of $\Delta R = 0.4$ around the π_ν line of flight as a function of the π_ν radial decay distance in the MS barrel and as a function of the $|z|$ decay coordinate in the MS end-caps. Figure 8 illustrates that a π_ν decaying in the MS results in a mean value of approximately three RoIs and from four to five RoIs clustered around the π_ν line of flight in the barrel and in the end-caps, respectively. The mean number of RoIs in the MS barrel is less than three RoIs for the sample with $m_H = 126$ GeV and $m_{\pi_\nu} = 10$ GeV due to the higher π_ν boost, which leads to narrower jets in the MS. For π_ν decays close to the end of the HCal ($r \sim 4$ m in the barrel and $|z| \sim 6$ m in the end-caps), the average number of muon RoIs contained in the cone increases rapidly due to the charged-particle tracks from the π_ν decay passing through the calorimeter and entering the MS. Once the π_ν decays occur in the MS, the number of RoIs remains approximately constant until the π_ν decays are close to the muon trigger plane ($r \sim 7$ m in the barrel and $|z| \sim 13$ m in the end-caps), at which point the charged hadrons are

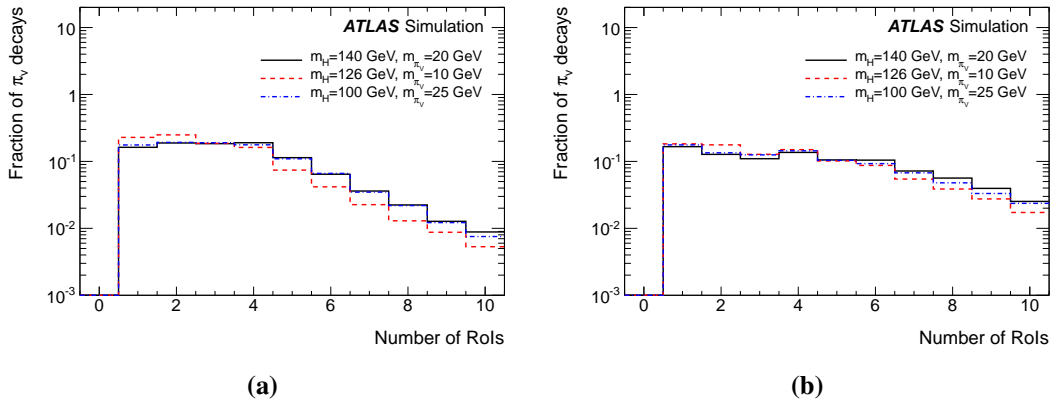


Figure 7. Distribution of the total number of RoIs found in events with a π_ν decaying in (a) the MS barrel and (b) the MS end-caps.

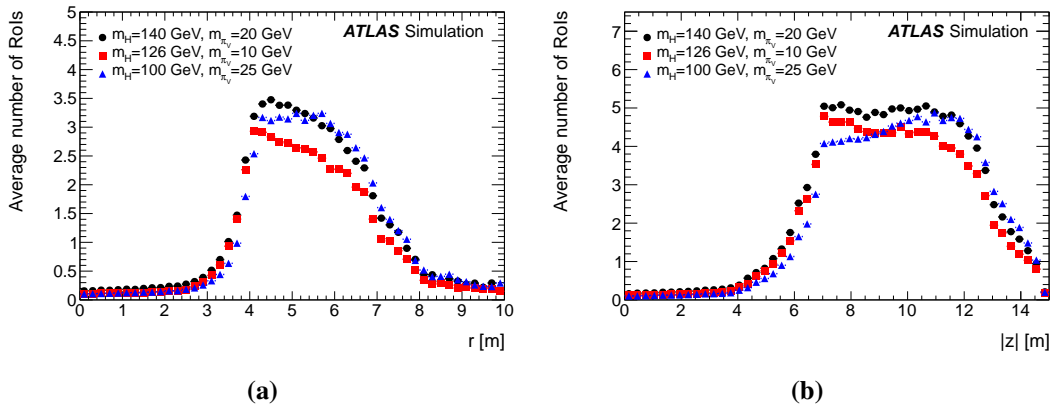


Figure 8. Average number of L1 muon RoIs in a cone of $\Delta R = 0.4$ around the π_ν line of flight as a function of (a) the π_ν radial decay position, r , in the MS barrel and (b) the $|z|$ coordinate of the π_ν decay in the MS end-caps.

not spatially separated enough to give multiple, unique RoIs. Moreover, decays occurring beyond the first trigger plane do not give RoIs because hits are required in both the first and second trigger planes.

A cluster of muon RoIs is defined as a $\Delta R = 0.4$ radius region in the MS barrel (end-caps) containing at least three (four) muon RoIs. This characteristic signature is exploited at the HLT to select events with π_ν decays at the outermost regions of the HCal or in the MS. The SM backgrounds from punch-through jets and bremsstrahlung from muons can be suppressed by requiring the RoI cluster to be isolated with respect to both calorimeter jets and tracks in the ID.

Figure 9(a) shows the fraction of events accepted as a function of the ΔR distance from the nearest jet to the RoI cluster centre in signal events. The acceptance is relatively flat up to values of $\Delta R \sim 0.7$. Requiring the muon RoI cluster to be isolated from jets within $\Delta R < 0.7$ results in a signal loss of less than $\sim 3\%$. It should be noted that the RoI cluster is only required to be isolated from jets that have $\log_{10}(E_{\text{HAD}}/E_{\text{EM}}) < 0.5$ in order to increase the signal efficiency for events in which the π_ν decays at the end of the HCal, depositing energy and thus producing both a jet with significant hadronic energy and a muon RoI cluster.

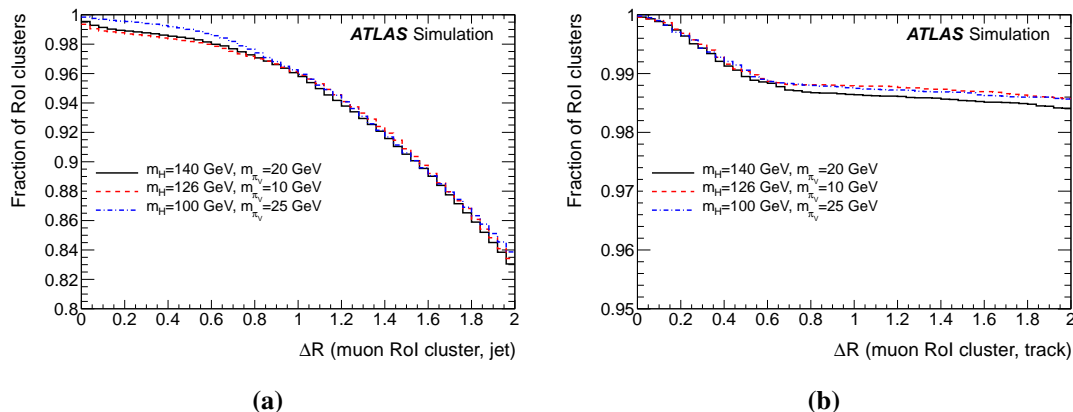


Figure 9. Fraction of RoI clusters accepted in signal events as a function of ΔR between (a) the centre of the RoI cluster and the jet direction for L2 jets with $\log_{10}(E_{\text{HAD}}/E_{\text{EM}}) < 0.5$ and (b) the centre of the RoI cluster and the track direction for L2 tracks with $p_{\text{T}} > 5$ GeV.

Figure 9(b) shows the fraction of events accepted at L2 as a function of ΔR between the centre of the RoI cluster and the nearest track in the ID with $p_{\text{T}} > 5$ GeV. Because the π_{ν} particles are both long lived, high- p_{T} tracks are not expected to be reconstructed in the ID. The acceptance is found to be approximately constant across a wide range of ΔR values. Requiring isolation within a region of $\Delta R < 0.4$ results in an acceptance loss of less than $\sim 1\%$.

The timing of the L1 muon trigger is centred on the arrival time of the bunch crossing in ATLAS, so that the trigger is active for 12.5 ns before and 12.5 ns after the bunch crossing. To ensure that the Muon RoI Cluster trigger is associated with the correct bunch crossing, the critical parameter to examine is the time delay between π_{ν} decays in the MS and a particle produced in the same interaction travelling with $\beta = 1$. The π_{ν} decay products have $\beta \simeq 1$. Thus, in determining the time delay between the π_{ν} arrival and a $\beta = 1$ particle, only the distance the π_{ν} travels from the IP to the decay point needs to be considered.

The efficiency of the RPC trigger was measured, as a function of the time shift Δt , in a test beam [15]. The RPC time resolution has also been measured for the 2011 data and found to be in good agreement with the test beam results. The L1 muon trigger accurately matches events to their bunch crossings for time delays of less than approximately 6 ns. Time delays beyond 6 ns result in some of the triggers being associated with the next bunch crossing in a predictable Gaussian manner. If the trigger signal from the π_{ν} is not associated with the correct bunch crossing, the event is lost.

The expected online acceptance of the L1 trigger in the barrel MS for the three benchmark mass points can be calculated⁴ from the measured bunch-crossing identification efficiency, given in ref. [15], and the β distribution of the π_{ν} . The results are shown in table 2 for π_{ν} particles emitted at $\eta = 0$ and $|\eta| = 1$. Similar results are obtained for the trigger system in the end-caps. The table also gives the trigger acceptances obtained from the simulation, which are systematically shifted to larger values because in the barrel trigger simulation at L1 there is a time shift of plus 3.125 ns (one

⁴The distances to the first muon trigger plane are used for the calculation of the online quantities: $L = 7$ m and $L = 11$ m for $\eta = 0$ and $|\eta| = 1$, respectively.

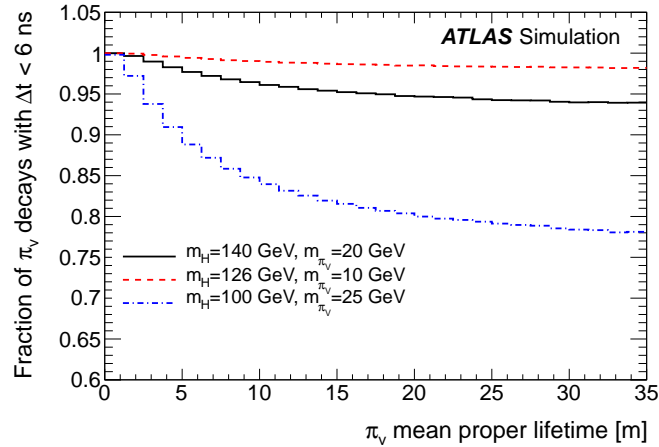


Figure 10. Fraction of π_ν decays producing a Muon RoI Cluster trigger associated with the correct bunch crossing as a function of the π_ν mean proper lifetime.

Table 2. The probability of associating π_ν particles emitted at $\eta = 0$ and $|\eta| = 1$ with the correct bunch crossing for both simulation and data for the three benchmark samples. The statistical uncertainties are negligible.

Sample	data eff. $\eta = 0$	MC eff. $\eta = 0$	data eff. $ \eta = 1$	MC eff. $ \eta = 1$
$m_H/m_{\pi_\nu} = 100/25$ GeV	94.4%	97.6%	88.9%	94.9%
$m_H/m_{\pi_\nu} = 126/10$ GeV	99.8%	99.9%	99.6%	99.8%
$m_H/m_{\pi_\nu} = 140/20$ GeV	98.9%	99.4%	97.9%	99.0%

least count) with respect to the online trigger. As a consequence, the simulation has a correctable, systematically higher acceptance for late trigger signals as shown in table 2 for the three benchmark samples. Analyses using this trigger will need to calculate the corrected efficiency.

Figure 10 shows the fraction of π_ν decays in the MS with a Δt of less than 6 ns as a function of the π_ν mean proper lifetime. These are decays that could produce a trigger associated with the correct bunch crossing. The π_ν is associated with the correct bunch crossing with an efficiency greater than 75% for the $m_H = 100$ GeV and $m_{\pi_\nu} = 25$ GeV sample and with an efficiency greater than 94% for the other mass points. When the mean proper decay length is small compared to the detector dimensions, only very boosted π_ν particles have non-negligible probability to decay in the MS. As the mean proper decay length increases, those π_ν particles with a smaller boost begin to have some probability to decay in the MS. When the mean proper decay length becomes comparable to the ATLAS detector dimensions all the π_ν particles have roughly equal probability to decay in the MS.

The Muon RoI Cluster trigger is built by requiring two muons with $p_T > 10$ GeV at L1. A cluster of muon RoIs is required at L2 for all the events passing the L1 selection. Then, the L2 jet and track reconstruction algorithms are employed using all the jet RoIs found in the same event. The jet isolation criterion is then applied, requiring that there be no jets within $\Delta R = 0.7$ around the muon RoI cluster centre with $E_T > 30$ GeV and $\log_{10}(E_{HAD}/E_{EM}) < 0.5$, where the calorimeter response is calibrated at the EM scale. The track isolation criterion is also applied, requiring no

tracks in the ID with $p_T > 5$ GeV within $\Delta R = 0.4$ of the muon RoI cluster centre. No further selection is applied at the EF. A schematic diagram of the sequence of algorithms employed in the Muon RoI Cluster trigger is depicted in figure 4(c).

7 Trigger efficiency on simulated events

The efficiency is defined as the fraction of π_ν particles that pass one of the triggers for displaced decays of long-lived neutral particles as a function of the π_ν decay position. Figures 11–13 show the long-lived neutral particle trigger efficiencies for the simulated mass points, with mean $\langle\mu\rangle = 22$, as a function of the π_ν decay position for decays in the barrel and end-cap regions of the ATLAS detector. The uncertainties shown are statistical only. The Calorimeter Ratio trigger and Muon RoI cluster triggers have good efficiency throughout the detector volume. All of the efficiencies are lower in the forward region than in the central region. In general, this is a consequence of events not satisfying the isolation criteria because of the higher mean occupancy in the forward region due to pile-up interactions.

The Trackless Jet trigger is less than 5% efficient for decays occurring in the region of the barrel between the middle of the ID and the ECal. The trigger efficiency increases as the decay occurs closer to the end of the HCal. The dependence of the efficiency on the decay position is a consequence of the low p_T distribution of muons produced by the π_ν decays. A muon originating in the ID will lose an average of 4 GeV of energy as it traverses the ATLAS calorimeters [16]; therefore, a larger fraction of muons produced in π_ν decays reach the muon system as the π_ν decays further into the calorimeter. The efficiency in the end-cap regions is ~ 1 –2%. The Calorimeter Ratio trigger is $\sim 25\%$ efficient for π_ν decays in the HCal barrel and 10% in the HCal end-caps. The Muon RoI Cluster trigger in the MS barrel is $\sim 40\%$ efficient from the end of the HCal to $r \sim 6$ m. The efficiency drops beyond a radial distance of 6 m because the jets originating from the π_ν decay do not separate sufficiently before reaching the first muon trigger plane located at $r \sim 7$ m. The trigger efficiency in the MS end-caps is 15–25% for $|z|$ between 7 and 12 m from the IP.

The lower efficiency of the Calorimeter Ratio trigger for the sample with $m_H = 100$ GeV and $m_{\pi_\nu} = 25$ GeV is due to the tight L1 energy threshold and the fact that jets produced by the π_ν decays in this MC sample have lower energies compared to the other samples. The lower efficiency of the Muon RoI Cluster trigger and rapid decrease with increasing decay distance for the sample with $m_H = 126$ GeV and $m_{\pi_\nu} = 10$ GeV is due to the higher π_ν boost that results in collinear jets that are more likely to be contained in a single MS sector. Because the L1 muon firmware is limited to no more than two RoIs per sector, many of these decays do not satisfy the trigger condition that requires three (four) or more RoIs in the MS barrel (end-caps). The effect is minimized if the jet axis falls between two adjacent MS sectors.

To evaluate the effect of pile-up interactions on the trigger efficiency, the MC samples are arbitrarily divided into two subsamples, one with $\langle\mu\rangle > 22$ and one with $\langle\mu\rangle \leq 22$, with mean $\langle\mu\rangle$ values of 28.6 and 15.8, respectively. Tables 3 and 4 give, for the three triggers, the ratio of Efficiency(28.6)/Efficiency(15.8) in the barrel and end-cap detectors.⁵ Both the Trackless Jet and the Calorimeter Ratio triggers show significant reduction of efficiency with increasing pile-up in both the barrel and end-cap regions. These two triggers are particularly sensitive to pile-up

⁵The efficiencies used in the ratio are averaged over the r and $|z|$ ranges given in tables 3 and 4, respectively.

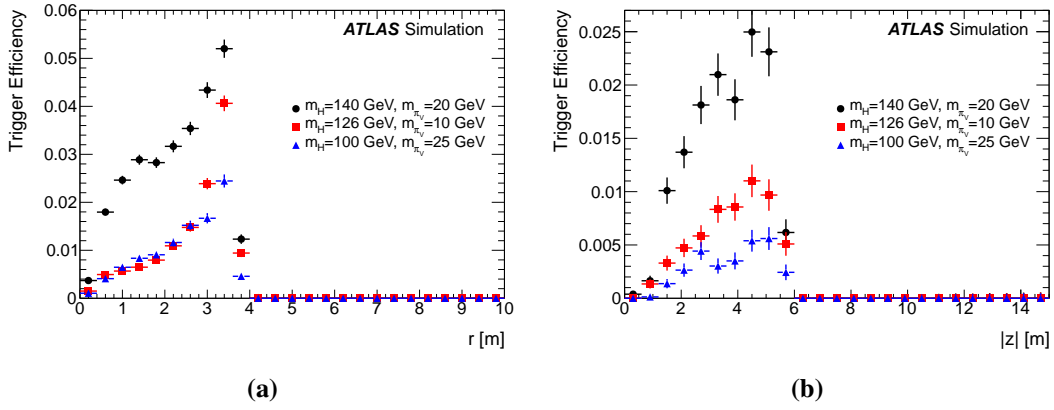


Figure 11. Efficiency for the Trackless Jet trigger as a function of (a) the radial decay position, r , for π_ν decays in the barrel and (b) the $|z|$ position for π_ν decays in the end-caps.

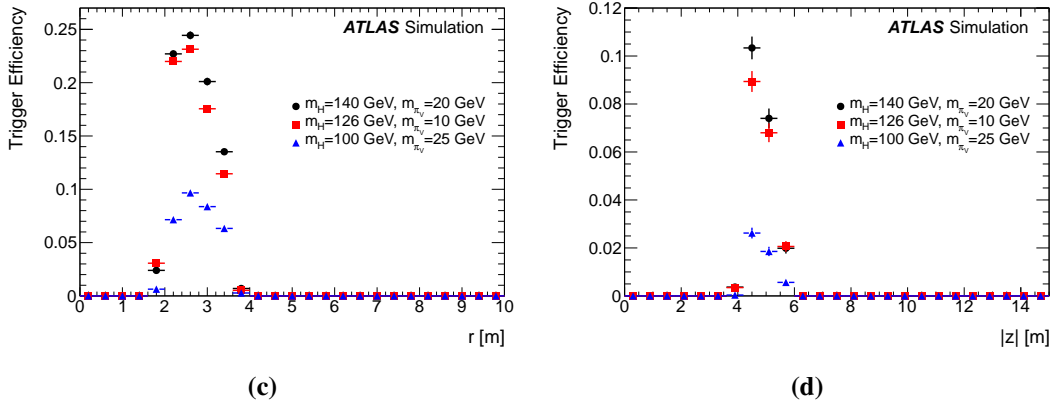


Figure 12. Efficiency for the Calorimeter Ratio trigger as a function of (a) the radial decay position, r , for π_ν decays in the barrel and (b) the $|z|$ position for π_ν decays in the end-caps.

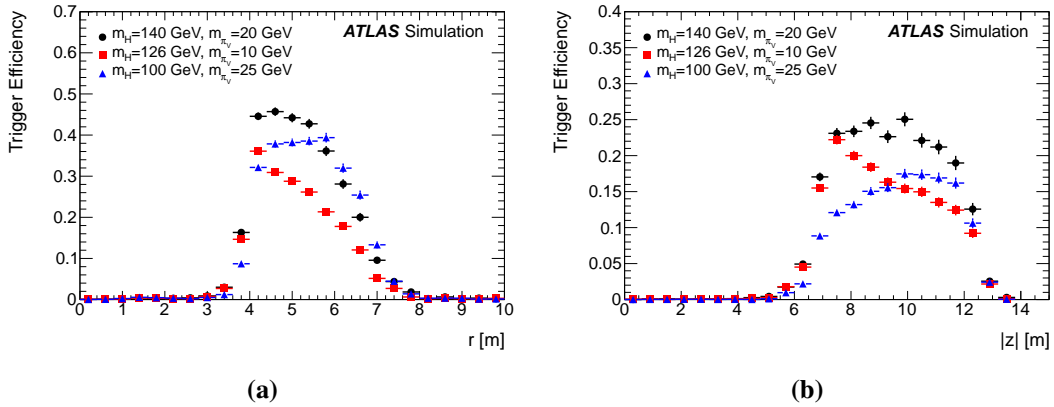


Figure 13. Efficiency for the Muon RoI Cluster trigger as a function of (a) the radial decay position, r , for π_ν decays in the barrel and (b) the $|z|$ position for π_ν decays in the end-caps.

Table 3. The ratio of the trigger efficiencies in the barrel for mean $\langle\mu\rangle = 28.6$ (high pile-up sample) to mean $\langle\mu\rangle = 15.8$ (low pile-up sample) for the three triggers and the three benchmark samples. The uncertainties shown are statistical only.

Sample	Trackless Jet	Calorimeter Ratio	Muon RoI Cluster	Range [m]
$m_{\text{H}}/m_{\pi_{\nu}} = 100/25$ GeV	0.70 ± 0.04	0.48 ± 0.04	1.03 ± 0.03	$0.4 < r < 4.0$
$m_{\text{H}}/m_{\pi_{\nu}} = 126/10$ GeV	0.76 ± 0.04	0.47 ± 0.02	0.95 ± 0.03	$2.0 < r < 4.0$
$m_{\text{H}}/m_{\pi_{\nu}} = 140/20$ GeV	0.64 ± 0.02	0.50 ± 0.02	0.98 ± 0.03	$4.0 < r < 7.2$

Table 4. The ratio of the trigger efficiencies in the end-caps for mean $\langle\mu\rangle = 28.6$ (high pile-up sample) to mean $\langle\mu\rangle = 15.8$ (low pile-up sample) for the three triggers and the three benchmark samples. The uncertainties shown are statistical only.

Sample	Trackless Jet	Calorimeter Ratio	Muon RoI Cluster	Range [m]
$m_{\text{H}}/m_{\pi_{\nu}} = 100/25$ GeV	0.32 ± 0.07	0.34 ± 0.06	0.93 ± 0.02	$1.8 < z < 6.0$
$m_{\text{H}}/m_{\pi_{\nu}} = 126/10$ GeV	0.51 ± 0.08	0.35 ± 0.03	0.93 ± 0.02	$4.2 < z < 6.0$
$m_{\text{H}}/m_{\pi_{\nu}} = 140/20$ GeV	0.39 ± 0.04	0.40 ± 0.04	0.92 ± 0.02	$6.0 < z < 13.2$

interactions because of the tight isolation criterion that requires no reconstructed tracks at L2 with $p_{\text{T}} > 0.8$ and $p_{\text{T}} > 1$ GeV in a cone around the jet axis for the Trackless Jet and Calorimeter Ratio triggers, respectively. The Muon RoI Cluster trigger includes a softer track isolation cut, no reconstructed tracks at L2 with $p_{\text{T}} > 5$ GeV around the muon RoI cluster centre, and is more robust against pile-up. No effect is observed in the barrel region while in the end-caps there is an approximate 7% reduction. The isolation cuts represent a compromise between maximizing the signal acceptance and reducing the final output rate to a sustainable level.

From the trigger efficiency plots, the signal fraction accepted by the long-lived neutral particle triggers is predicted as a function of the π_{ν} mean proper lifetime. The fraction of π_{ν} decays that occur at a certain radius is weighted by the corresponding trigger efficiency for the same radius. Figure 14 shows the expected fraction of events that pass each trigger as a function of the π_{ν} mean proper lifetime for $m_{\text{H}} = 140$ GeV and $m_{\pi_{\nu}} = 20$ GeV.

All the trigger studies and efficiencies presented in this paper are based on MC simulations and the associated uncertainties are statistical only. An analysis using one or more of these triggers will need to make a careful study of the systematic uncertainties. While the details of the study are analysis dependent, standard sources of systematic uncertainties include the jet energy scale, the jet energy resolution, the modelling of hard and soft proton-proton interactions and the instantaneous luminosity. Additional systematic uncertainty studies that focus on the physics objects used by these triggers need to be taken into account and some examples follow.

The cluster of muon RoIs resulting from a π_{ν} decay in the MS is the basic physics object used by the Muon RoI Cluster trigger. To compare the MS detector response to a π_{ν} decay in data and simulation, a sample of jets that punch through the calorimeter can be used. The punch-through jets are similar to signal events in that both low- p_{T} photons and charged hadrons are present in a narrow region of the MS, thus the detector response to such an environment can be verified between data and simulation. The systematic uncertainty related to the logarithmic ratio selection criteria can be

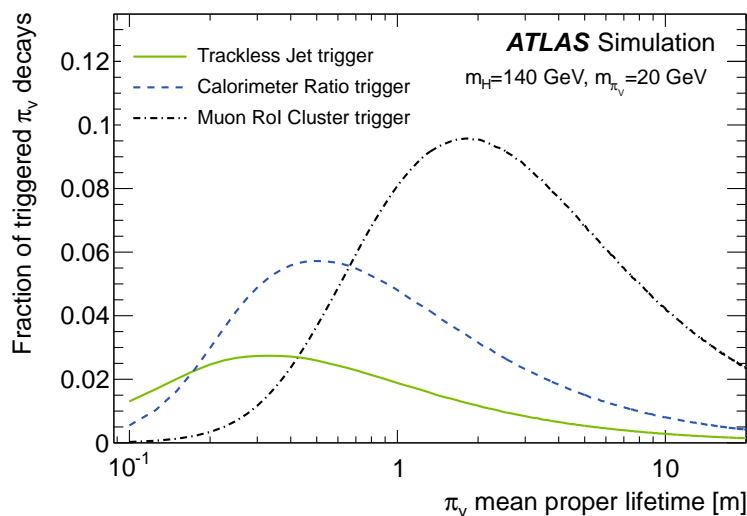


Figure 14. The expected fraction of events that pass each of the long-lived neutral particle triggers as a function of the π_0 mean proper lifetime.

studied by selecting a sample of jets with a small fraction of energy in the ECal and comparing the distribution in data and simulation when applying the various cuts used in the Calorimeter Ratio trigger. For the Trackless Jet trigger, a data sample collected with a minimum bias trigger can be used to identify secondary vertex interactions that may mimic the decay topology of a π_0 in the ID or ECal. In general, systematic uncertainties are analysis dependent and detailed studies are beyond the scope of this paper.

8 Triggering on collision data

These triggers need to meet tight bandwidth requirements for inclusion in the ATLAS trigger menu. The exclusive bandwidth allocated for the long-lived neutral particle triggers is only a few Hz. Figure 15 shows the rates as a function of instantaneous luminosity for the three triggers during a typical 2012 data-taking period and demonstrates that the rates are well within the allocated trigger bandwidth. The Muon RoI Cluster trigger shows a linear dependence on the instantaneous luminosity. A linear fit, when extrapolated to null luminosity and accounting for the different number of filled and empty bunches, predicts a rate of (0.04 ± 0.01) Hz. An analogous trigger only enabled on empty bunch crossings gives a rate of (0.04 ± 0.03) Hz in the same data-taking period as that displayed in figure 15. The rates are found to be in excellent agreement, suggesting that the Muon RoI Cluster trigger rate increases linearly as a function of the instantaneous luminosity and there are no other dependencies affecting its rate.

The Trackless Jet and Calorimeter Ratio trigger rates show little or no dependence on the instantaneous luminosity. As discussed in the previous section, this is the result of the tight track isolation requirement included among the online selection cuts. The Muon RoI Cluster trigger uses a softer track isolation requirement and its rate is determined only by the instantaneous luminosity.

More detailed studies on data are, in general, not possible since the instantaneous luminosity and pile-up are correlated quantities and the LHC running conditions do not provide different

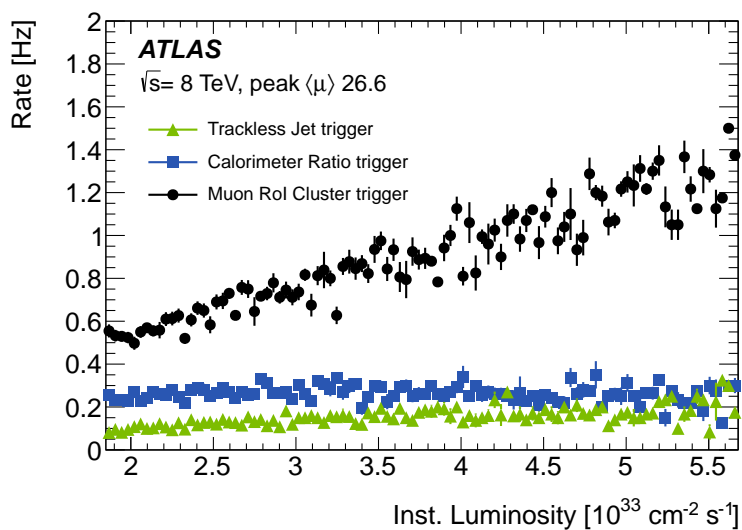


Figure 15. Trigger output rates as a function of the instantaneous luminosity during a typical 2012 data-taking period.

samples with the same instantaneous luminosity and different pile-up configurations. However, the correlation between the track isolation criterion and the amount of pile-up in the event can be further studied using the Muon RoI Cluster trigger. Figure 16 shows the ratio of the Muon RoI Cluster trigger rates as a function of $\langle\mu\rangle$ when lowering the threshold of the p_T tracking isolation cut below the nominal $p_T > 5$ GeV used in the trigger. There is no difference in the rate when requiring isolation using tracks with $p_T > 5$ GeV or $p_T > 3$ GeV. However, a net linear rate reduction with increasing pile-up is observed when using tracks with $p_T > 1$ GeV. As expected, a higher number of interactions per event increases the likelihood that the event is rejected for triggers using low-momentum track isolation.

9 Conclusions

Three signature-driven triggers designed to select decays of long-lived neutral particles throughout the ATLAS detector volume are described: the Trackless Jet trigger for decays beyond the pixel layers to the ECal, the Calorimeter Ratio trigger for decays in the HCal and the Muon RoI Cluster trigger for decays from the end of the HCal to the MS middle station. These triggers are demonstrated to be efficient for pairs of π_ν particles produced in Higgs boson decays, using different lifetimes and a range of Higgs boson and π_ν masses. They also met the tight bandwidth requirements of the ATLAS triggers during the 2012 LHC physics data-taking period. The estimated fraction of triggered π_ν particles is between 2% and 10% for a π_ν mean proper lifetime in the range 0.1 m to 20 m. The ATLAS physics potential for probing various SM extensions can be greatly extended using the triggers described in this paper.

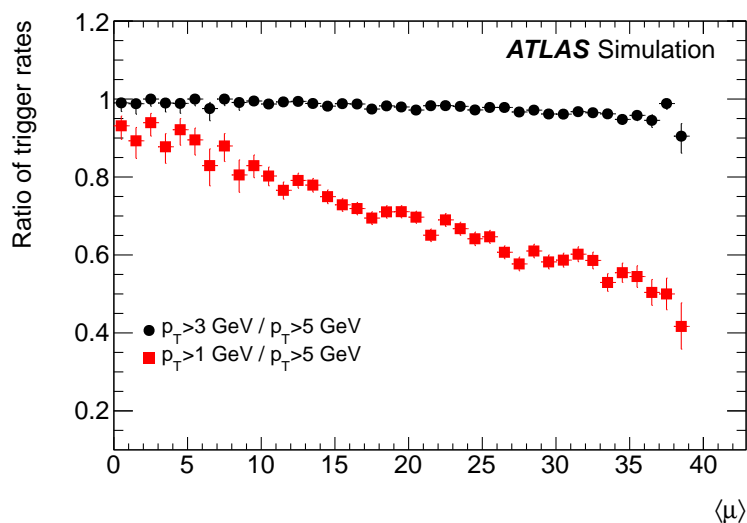


Figure 16. Ratio of trigger rates as a function of $\langle \mu \rangle$ when using lower p_T isolation cuts for the Muon RoI Cluster trigger compared to the $p_T > 5$ GeV cut used online.

Acknowledgments

We thank CERN for the very successful operation of the LHC, as well as the support staff from our institutions without whom ATLAS could not be operated efficiently.

We acknowledge the support of ANPCyT, Argentina; YerPhI, Armenia; ARC, Australia; BMWF and FWF, Austria; ANAS, Azerbaijan; SSTC, Belarus; CNPq and FAPESP, Brazil; NSERC, NRC and CFI, Canada; CERN; CONICYT, Chile; CAS, MOST and NSFC, China; COLCIENCIAS, Colombia; MSMT CR, MPO CR and VSC CR, Czech Republic; DNRF, DNSRC and Lundbeck Foundation, Denmark; EPLANET, ERC and NSRF, European Union; IN2P3-CNRS, CEA-DSM/IRFU, France; GNSF, Georgia; BMBF, DFG, HGF, MPG and AvH Foundation, Germany; GSRT and NSRF, Greece; ISF, MINERVA, GIF, DIP and Benoziyo Center, Israel; INFN, Italy; MEXT and JSPS, Japan; CNRST, Morocco; FOM and NWO, Netherlands; BRF and RCN, Norway; MNiSW, Poland; GRICES and FCT, Portugal; MERYS (MECTS), Romania; MES of Russia and ROSATOM, Russian Federation; JINR; MSTD, Serbia; MSSR, Slovakia; ARRS and MIZŠ, Slovenia; DST/NRF, South Africa; MICINN, Spain; SRC and Wallenberg Foundation, Sweden; SER, SNSF and Cantons of Bern and Geneva, Switzerland; NSC, Taiwan; TAEK, Turkey; STFC, the Royal Society and Leverhulme Trust, United Kingdom; DOE and NSF, United States of America.

The crucial computing support from all WLCG partners is acknowledged gratefully, in particular from CERN and the ATLAS Tier-1 facilities at TRIUMF (Canada), NDGF (Denmark, Norway, Sweden), CC-IN2P3 (France), KIT/GridKA (Germany), INFN-CNAF (Italy), NL-T1 (Netherlands), PIC (Spain), ASGC (Taiwan), RAL (UK) and BNL (USA) and in the Tier-2 facilities worldwide.

References

- [1] S. Dimopoulos, M. Dine, S. Raby and S.D. Thomas, *Experimental signatures of low-energy gauge mediated supersymmetry breaking*, *Phys. Rev. Lett.* **76** (1996) 3494 [[hep-ph/9601367](#)].
- [2] R. Barbier, C. Berat, M. Besancon, M. Chemtob, A. Deandrea et al., *R-parity violating supersymmetry*, *Phys. Rept.* **420** (2005) 1 [[hep-ph/0406039](#)].
- [3] D. Tucker-Smith and N. Weiner, *Inelastic dark matter*, *Phys. Rev. D* **64** (2001) 043502 [[hep-ph/0101138](#)].
- [4] M.J. Strassler and K.M. Zurek, *Echoes of a hidden valley at hadron colliders*, *Phys. Lett. B* **651** (2007) 374 [[hep-ph/0604261](#)].
- [5] M.J. Strassler and K.M. Zurek, *Discovering the Higgs through highly-displaced vertices*, *Phys. Lett. B* **661** (2008) 263 [[hep-ph/0605193](#)].
- [6] M.J. Strassler, *Possible effects of a hidden valley on supersymmetric phenomenology*, [hep-ph/0607160](#).
- [7] ATLAS collaboration, *Search for a light Higgs boson decaying to long-lived weakly-interacting particles in proton-proton collisions at $\sqrt{s} = 7$ TeV with the ATLAS detector*, *Phys. Rev. Lett.* **108** (2012) 251801 [[arXiv:1203.1303](#)].
- [8] ATLAS collaboration, *The ATLAS Experiment at the CERN Large Hadron Collider*, 2008 *JINST* **3** S08003.
- [9] ATLAS collaboration, *Performance of the ATLAS Trigger System in 2010*, *Eur. Phys. J. C* **72** (2012) 1849 [[arXiv:1110.1530](#)].
- [10] T. Sjöstrand, S. Mrenna and P.Z. Skands, *A Brief Introduction to PYTHIA 8.1*, *Comput. Phys. Commun.* **178** (2008) 852 [[arXiv:0710.3820](#)].
- [11] A. Martin, W. Stirling, R. Thorne and G. Watt, *Parton distributions for the LHC*, *Eur. Phys. J. C* **63** (2009) 189 [[arXiv:0901.0002](#)].
- [12] E. Fullana et al., *Digital Signal Reconstruction in the ATLAS Hadronic Tile Calorimeter*, *IEEE Trans. Nucl. Sci.* **53** (2006) 4.
- [13] ATLAS collaboration, *Implementation and performance of the signal reconstruction in the ATLAS Hadronic Tile Calorimeter*, [TILECAL-PROC-2011-008](#) (2011).
- [14] M. Cacciari, G.P. Salam and G. Soyez, *The Anti- k_t jet clustering algorithm*, *JHEP* **04** (2008) 063 [[arXiv:0802.1189](#)].
- [15] C. Adorisio et al., *System test of the ATLAS muon spectrometer in the H8 beam at the CERN SPS*, *Nucl. Instrum. Meth. A* **593** (2008) 232.
- [16] ATLAS collaboration, *Expected Performance of the ATLAS Experiment - Detector, Trigger and Physics*, [arXiv:0901.0512](#).

The ATLAS collaboration

G. Aad⁴⁸, T. Abajyan²¹, B. Abbott¹¹², J. Abdallah¹², S. Abdel Khalek¹¹⁶, A.A. Abdelalim⁴⁹, O. Abdinov¹¹, R. Aben¹⁰⁶, B. Abi¹¹³, M. Abolins⁸⁹, O.S. AbouZeid¹⁵⁹, H. Abramowicz¹⁵⁴, H. Abreu¹³⁷, Y. Abulaiti^{147a,147b}, B.S. Acharya^{165a,165b,a}, L. Adamczyk^{38a}, D.L. Adams²⁵, T.N. Addy⁵⁶, J. Adelman¹⁷⁷, S. Adomeit⁹⁹, T. Adye¹³⁰, S. Aefsky²³, J.A. Aguilar-Saavedra^{125b,b}, M. Agustoni¹⁷, S.P. Ahlen²², F. Ahles⁴⁸, A. Ahmad¹⁴⁹, M. Ahsan⁴¹, G. Aielli^{134a,134b}, T.P.A. Åkesson⁸⁰, G. Akimoto¹⁵⁶, A.V. Akimov⁹⁵, M.A. Alam⁷⁶, J. Albert¹⁷⁰, S. Albrand⁵⁵, M.J. Alconada Verzini⁷⁰, M. Aleksa³⁰, I.N. Aleksandrov⁶⁴, F. Alessandria^{90a}, C. Alexa^{26a}, G. Alexander¹⁵⁴, G. Alexandre⁴⁹, T. Alexopoulos¹⁰, M. Alhroob^{165a,165c}, M. Aliev¹⁶, G. Alimonti^{90a}, J. Alison³¹, B.M.M. Allbrooke¹⁸, L.J. Allison⁷¹, P.P. Allport⁷³, S.E. Allwood-Spiers⁵³, J. Almond⁸³, A. Aloisio^{103a,103b}, R. Alon¹⁷³, A. Alonso³⁶, F. Alonso⁷⁰, A. Altheimer³⁵, B. Alvarez Gonzalez⁸⁹, M.G. Alviggi^{103a,103b}, K. Amako⁶⁵, Y. Amaral Coutinho^{24a}, C. Amelung²³, V.V. Ammosov^{129,*}, S.P. Amor Dos Santos^{125a}, A. Amorim^{125a,c}, S. Amoroso⁴⁸, N. Amram¹⁵⁴, C. Anastopoulos³⁰, L.S. Ancu¹⁷, N. Andari³⁰, T. Andeen³⁵, C.F. Anders^{58b}, G. Anders^{58a}, K.J. Anderson³¹, A. Andreazza^{90a,90b}, V. Andrei^{58a}, X.S. Anduaga⁷⁰, S. Angelidakis⁹, P. Anger⁴⁴, A. Angerami³⁵, F. Anghinolfi³⁰, A. Anisenkov¹⁰⁸, N. Anjos^{125a}, A. Annovi⁴⁷, A. Antonaki⁹, M. Antonelli⁴⁷, A. Antonov⁹⁷, J. Antos^{145b}, F. Anulli^{133a}, M. Aoki¹⁰², L. Aperio Bella¹⁸, R. Apolle^{119,d}, G. Arabidze⁸⁹, I. Aracena¹⁴⁴, Y. Arai⁶⁵, A.T.H. Arce⁴⁵, S. Arfaoui¹⁴⁹, J-F. Arguin⁹⁴, S. Argyropoulos⁴², E. Arik^{19a,*}, M. Arik^{19a}, A.J. Armbruster⁸⁸, O. Arnaez⁸², V. Arnal⁸¹, A. Artamonov⁹⁶, G. Artoni^{133a,133b}, D. Arutinov²¹, S. Asai¹⁵⁶, N. Asbah⁹⁴, S. Ask²⁸, B. Åsman^{147a,147b}, L. Asquith⁶, K. Assamagan²⁵, R. Astalos^{145a}, A. Astbury¹⁷⁰, M. Atkinson¹⁶⁶, B. Auerbach⁶, E. Auge¹¹⁶, K. Augsten¹²⁷, M. Aurousseau^{146b}, G. Avolio³⁰, D. Axen¹⁶⁹, G. Azuelos^{94,e}, Y. Azuma¹⁵⁶, M.A. Baak³⁰, G. Baccaglioni^{90a}, C. Bacci^{135a,135b}, A.M. Bach¹⁵, H. Bachacou¹³⁷, K. Bachas¹⁵⁵, M. Backes⁴⁹, M. Backhaus²¹, J. Backus Mayes¹⁴⁴, E. Badescu^{26a}, P. Bagiacci^{133a,133b}, P. Bagnaia^{133a,133b}, Y. Bai^{33a}, D.C. Bailey¹⁵⁹, T. Bain³⁵, J.T. Baines¹³⁰, O.K. Baker¹⁷⁷, S. Baker⁷⁷, P. Balek¹²⁸, F. Balli¹³⁷, E. Banas³⁹, P. Banerjee⁹⁴, Sw. Banerjee¹⁷⁴, D. Banfi³⁰, A. Bangert¹⁵¹, V. Bansal¹⁷⁰, H.S. Bansil¹⁸, L. Barak¹⁷³, S.P. Baranov⁹⁵, T. Barber⁴⁸, E.L. Barberio⁸⁷, D. Barberis^{50a,50b}, M. Barbero⁸⁴, D.Y. Bardin⁶⁴, T. Barillari¹⁰⁰, M. Barisonzi¹⁷⁶, T. Barklow¹⁴⁴, N. Barlow²⁸, B.M. Barnett¹³⁰, R.M. Barnett¹⁵, A. Baroncelli^{135a}, G. Barone⁴⁹, A.J. Barr¹¹⁹, F. Barreiro⁸¹, J. Barreiro Guimarães da Costa⁵⁷, R. Bartoldus¹⁴⁴, A.E. Barton⁷¹, V. Bartsch¹⁵⁰, A. Basye¹⁶⁶, R.L. Bates⁵³, L. Batkova^{145a}, J.R. Batley²⁸, A. Battaglia¹⁷, M. Battistin³⁰, F. Bauer¹³⁷, H.S. Bawa^{144,f}, S. Beale⁹⁹, T. Beau⁷⁹, P.H. Beauchemin¹⁶², R. Beccherle^{50a}, P. Bechtel²¹, H.P. Beck¹⁷, K. Becker¹⁷⁶, S. Becker⁹⁹, M. Beckingham¹³⁹, K.H. Becks¹⁷⁶, A.J. Beddall^{19c}, A. Beddall^{19c}, S. Bedikian¹⁷⁷, V.A. Bednyakov⁶⁴, C.P. Bee⁸⁴, L.J. Beemster¹⁰⁶, T.A. Beermann¹⁷⁶, M. Begel²⁵, C. Belanger-Champagne⁸⁶, P.J. Bell⁴⁹, W.H. Bell⁴⁹, G. Bella¹⁵⁴, L. Bellagamba^{20a}, A. Bellerive²⁹, M. Bellomo³⁰, A. Belloni⁵⁷, O. Beloborodova^{108,g}, K. Belotskiy⁹⁷, O. Beltramello³⁰, O. Benary¹⁵⁴, D. Benchechroun^{136a}, K. Bendtz^{147a,147b}, N. Benekos¹⁶⁶, Y. Benhammou¹⁵⁴, E. Benhar Noccioli⁴⁹, J.A. Benitez Garcia^{160b}, D.P. Benjamin⁴⁵, J.R. Bensinger²³, K. Benslama¹³¹, S. Bentvelsen¹⁰⁶, D. Berge³⁰, E. Bergeas Kuutmann¹⁶, N. Berger⁵, F. Berghaus¹⁷⁰, E. Berglund¹⁰⁶, J. Beringer¹⁵, P. Bernat⁷⁷, R. Bernhard⁴⁸, C. Bernius⁷⁸, F.U. Bernlochner¹⁷⁰, T. Berry⁷⁶, C. Bertella⁸⁴, F. Bertolucci^{123a,123b}, M.I. Besana^{90a,90b}, G.J. Besjes¹⁰⁵, N. Besson¹³⁷, S. Bethke¹⁰⁰, W. Bhimji⁴⁶, R.M. Bianchi³⁰, L. Bianchini²³, M. Bianco^{72a,72b}, O. Biebel⁹⁹, S.P. Bieniek⁷⁷, K. Bierwagen⁵⁴, J. Biesiada¹⁵, M. Biglietti^{135a}, H. Bilokon⁴⁷, M. Bindi^{20a,20b}, S. Binet¹¹⁶, A. Bingul^{19c}, C. Bini^{133a,133b}, B. Bittner¹⁰⁰, C.W. Black¹⁵¹, J.E. Black¹⁴⁴, K.M. Black²², D. Blackburn¹³⁹, R.E. Blair⁶, J.-B. Blanchard¹³⁷, T. Blazek^{145a}, I. Bloch⁴², C. Blocker²³, J. Blocki³⁹, W. Blum⁸², U. Blumenschein⁵⁴, G.J. Bobbink¹⁰⁶, V.S. Bobrovnikov¹⁰⁸, S.S. Bocchetta⁸⁰, A. Bocci⁴⁵, C.R. Boddy¹¹⁹, M. Boehler⁴⁸, J. Boek¹⁷⁶, T.T. Boek¹⁷⁶, N. Boelaert³⁶, J.A. Bogaerts³⁰, A. Bogdanchikov¹⁰⁸, A. Bogouch^{91,*}, C. Bohm^{147a}, J. Bohm¹²⁶, V. Boisvert⁷⁶, T. Bold^{38a}, V. Boldea^{26a}, N.M. Bolnet¹³⁷, M. Bomben⁷⁹, M. Bona⁷⁵, M. Boonekamp¹³⁷, S. Bordini⁷⁹, C. Borer¹⁷, A. Borisov¹²⁹, G. Borissov⁷¹, M. Borri⁸³,

S. Borroni⁴², J. Bortfeldt⁹⁹, V. Bortolotto^{135a,135b}, K. Bos¹⁰⁶, D. Boscherini^{20a}, M. Bosman¹², H. Boterenbrood¹⁰⁶, J. Bouchami⁹⁴, J. Boudreau¹²⁴, E.V. Bouhova-Thacker⁷¹, D. Boumediene³⁴, C. Bourdarios¹¹⁶, N. Bousson⁸⁴, S. Boutouil^{136d}, A. Boveia³¹, J. Boyd³⁰, I.R. Boyko⁶⁴, I. Bozovic-Jelisavcic^{13b}, J. Bracinik¹⁸, P. Branchini^{135a}, A. Brandt⁸, G. Brandt¹⁵, O. Brandt⁵⁴, U. Bratzler¹⁵⁷, B. Brau⁸⁵, J.E. Brau¹¹⁵, H.M. Braun^{176,*}, S.F. Brazzale^{165a,165c}, B. Brelrier¹⁵⁹, J. Bremer³⁰, K. Brendlinger¹²¹, R. Brenner¹⁶⁷, S. Bressler¹⁷³, T.M. Bristow^{146c}, D. Britton⁵³, F.M. Brochu²⁸, I. Brock²¹, R. Brock⁸⁹, F. Broggi^{90a}, C. Bromberg⁸⁹, J. Bronner¹⁰⁰, G. Brooijmans³⁵, T. Brooks⁷⁶, W.K. Brooks^{32b}, E. Brost¹¹⁵, G. Brown⁸³, P.A. Bruckman de Renstrom³⁹, D. Bruncko^{145b}, R. Bruneliere⁴⁸, S. Brunet⁶⁰, A. Bruni^{20a}, G. Bruni^{20a}, M. Bruschi^{20a}, L. Bryngemark⁸⁰, T. Buanes¹⁴, Q. Buat⁵⁵, F. Buccini⁴⁹, J. Buchanan¹¹⁹, P. Buchholz¹⁴², R.M. Buckingham¹¹⁹, A.G. Buckley⁴⁶, S.I. Buda^{26a}, I.A. Budagov⁶⁴, B. Budick¹⁰⁹, L. Bugge¹¹⁸, O. Bulekov⁹⁷, A.C. Bundock⁷³, M. Bunse⁴³, T. Buran^{118,*}, H. Burckhart³⁰, S. Burdin⁷³, T. Burgess¹⁴, S. Burke¹³⁰, E. Busato³⁴, V. Büscher⁸², P. Bussey⁵³, C.P. Buszello¹⁶⁷, B. Butler⁵⁷, J.M. Butler²², C.M. Buttar⁵³, J.M. Butterworth⁷⁷, W. Buttinger²⁸, M. Byszewski¹⁰, S. Cabrera Urbán¹⁶⁸, D. Caforio^{20a,20b}, O. Cakir^{4a}, P. Calafiura¹⁵, G. Calderini⁷⁹, P. Calfayan⁹⁹, R. Calkins¹⁰⁷, L.P. Caloba^{24a}, R. Caloi^{133a,133b}, D. Calvet³⁴, S. Calvet³⁴, R. Camacho Toro⁴⁹, P. Camarri^{134a,134b}, D. Cameron¹¹⁸, L.M. Caminada¹⁵, R. Caminal Armadans¹², S. Campana³⁰, M. Campanelli⁷⁷, V. Canale^{103a,103b}, F. Canelli³¹, A. Canepa^{160a}, J. Cantero⁸¹, R. Cantrill⁷⁶, T. Cao⁴⁰, M.D.M. Capeans Garrido³⁰, I. Caprini^{26a}, M. Caprini^{26a}, D. Capriotti¹⁰⁰, M. Capua^{37a,37b}, R. Caputo⁸², R. Cardarelli^{134a}, T. Carli³⁰, G. Carlino^{103a}, L. Carminati^{90a,90b}, S. Caron¹⁰⁵, E. Carquin^{32b}, G.D. Carrillo-Montoya^{146c}, A.A. Carter⁷⁵, J.R. Carter²⁸, J. Carvalho^{125a,h}, D. Casadei¹⁰⁹, M.P. Casado¹², M. Cascella^{123a,123b}, C. Caso^{50a,50b,*}, E. Castaneda-Miranda¹⁷⁴, A. Castelli¹⁰⁶, V. Castillo Gimenez¹⁶⁸, N.F. Castro^{125a}, G. Cataldi^{72a}, P. Catastini⁵⁷, A. Catinaccio³⁰, J.R. Catmore³⁰, A. Cattai³⁰, G. Cattani^{134a,134b}, S. Caughron⁸⁹, V. Cavaliere¹⁶⁶, D. Cavalli^{90a}, M. Cavalli-Sforza¹², V. Cavasinni^{123a,123b}, F. Ceradini^{135a,135b}, B. Cerio⁴⁵, A.S. Cerqueira^{24b}, A. Cerri¹⁵, L. Cerrito⁷⁵, F. Cerutti¹⁵, A. Cervelli¹⁷, S.A. Cetin^{19b}, A. Chafaq^{136a}, D. Chakraborty¹⁰⁷, I. Chalupkova¹²⁸, K. Chan³, P. Chang¹⁶⁶, B. Chapleau⁸⁶, J.D. Chapman²⁸, J.W. Chapman⁸⁸, D.G. Charlton¹⁸, V. Chavda⁸³, C.A. Chavez Barajas³⁰, S. Cheatham⁸⁶, S. Chekanov⁶, S.V. Chekulaev^{160a}, G.A. Chelkov⁶⁴, M.A. Chelstowska¹⁰⁵, C. Chen⁶³, H. Chen²⁵, S. Chen^{33c}, X. Chen¹⁷⁴, Y. Chen³⁵, Y. Cheng³¹, A. Cheplakov⁶⁴, R. Cherkaoui El Moursli^{136e}, V. Chernyatin²⁵, E. Cheu⁷, S.L. Cheung¹⁵⁹, L. Chevalier¹³⁷, V. Chiarella⁴⁷, G. Chiefari^{103a,103b}, J.T. Childers³⁰, A. Chilingarov⁷¹, G. Chiodini^{72a}, A.S. Chisholm¹⁸, R.T. Chislett⁷⁷, A. Chitan^{26a}, M.V. Chizhov⁶⁴, G. Choudalakis³¹, S. Chouridou⁹, B.K.B. Chow⁹⁹, I.A. Christidi⁷⁷, A. Christov⁴⁸, D. Chromek-Burckhart³⁰, M.L. Chu¹⁵², J. Chudoba¹²⁶, G. Ciapetti^{133a,133b}, A.K. Ciftci^{4a}, R. Ciftci^{4a}, D. Cinca⁶², V. Cindro⁷⁴, A. Ciocio¹⁵, M. Cirilli⁸⁸, P. Cirkovic^{13b}, Z.H. Citron¹⁷³, M. Citterio^{90a}, M. Ciubancan^{26a}, A. Clark⁴⁹, P.J. Clark⁴⁶, R.N. Clarke¹⁵, J.C. Clemens⁸⁴, B. Clement⁵⁵, C. Clement^{147a,147b}, Y. Coadou⁸⁴, M. Cokal^{165a,165c}, A. Coccaro¹³⁹, J. Cochran⁶³, S. Coelli^{90a}, L. Coffey²³, J.G. Cogan¹⁴⁴, J. Coggeshall¹⁶⁶, J. Colas⁵, S. Cole¹⁰⁷, A.P. Colijn¹⁰⁶, N.J. Collins¹⁸, C. Collins-Tooth⁵³, J. Collot⁵⁵, T. Colombo^{120a,120b}, G. Colon⁸⁵, G. Compostella¹⁰⁰, P. Conde Muiño^{125a}, E. Coniavitis¹⁶⁷, M.C. Conidi¹², S.M. Consonni^{90a,90b}, V. Consorti⁴⁸, S. Constantinescu^{26a}, C. Conta^{120a,120b}, G. Conti⁵⁷, F. Conventi^{103a,i}, M. Cooke¹⁵, B.D. Cooper⁷⁷, A.M. Cooper-Sarkar¹¹⁹, N.J. Cooper-Smith⁷⁶, K. Copic¹⁵, T. Cornelissen¹⁷⁶, M. Corradi^{20a}, F. Corriveau^{86,j}, A. Corso-Radu¹⁶⁴, A. Cortes-Gonzalez¹⁶⁶, G. Cortiana¹⁰⁰, G. Costa^{90a}, M.J. Costa¹⁶⁸, D. Costanzo¹⁴⁰, D. Côté³⁰, G. Cottin^{32a}, L. Courneyea¹⁷⁰, G. Cowan⁷⁶, B.E. Cox⁸³, K. Cranmer¹⁰⁹, S. Crépe-Renaudin⁵⁵, F. Crescioli⁷⁹, M. Cristinziani²¹, G. Crosetti^{37a,37b}, C.-M. Cuciuc^{26a}, C. Cuenca Almenar¹⁷⁷, T. Cuhadar Donszelmann¹⁴⁰, J. Cummings¹⁷⁷, M. Curatolo⁴⁷, C.J. Curtis¹⁸, C. Cuthbert¹⁵¹, H. Czirr¹⁴², P. Czodrowski⁴⁴, Z. Czyczula¹⁷⁷, S. D'Auria⁵³, M. D'Onofrio⁷³, A. D'Orazio^{133a,133b}, M.J. Da Cunha Sargedas De Sousa^{125a}, C. Da Via⁸³, W. Dabrowski^{38a}, A. Dafinca¹¹⁹, T. Dai⁸⁸, F. Dallaire⁹⁴, C. Dallapiccola⁸⁵, M. Dam³⁶, D.S. Damiani¹³⁸, A.C. Daniells¹⁸, H.O. Danielsson³⁰, V. Dao¹⁰⁵, G. Darbo^{50a}, G.L. Darlea^{26c}, S. Darmora⁸, J.A. Dassoulas⁴², W. Davey²¹, T. Davidek¹²⁸, N. Davidson⁸⁷, E. Davies^{119,d}, M. Davies⁹⁴, O. Davignon⁷⁹,

A.R. Davison⁷⁷, Y. Davygora^{58a}, E. Dawe¹⁴³, I. Dawson¹⁴⁰, R.K. Daya-Ishmukhametova²³, K. De⁸,
 R. de Asmundis^{103a}, S. De Castro^{20a,20b}, S. De Cecco⁷⁹, J. de Graat⁹⁹, N. De Groot¹⁰⁵, P. de Jong¹⁰⁶,
 C. De La Taille¹¹⁶, H. De la Torre⁸¹, F. De Lorenzi⁶³, L. De Nooij¹⁰⁶, D. De Pedis^{133a}, A. De Salvo^{133a},
 U. De Sanctis^{165a,165c}, A. De Santo¹⁵⁰, J.B. De Vivie De Regie¹¹⁶, G. De Zorzi^{133a,133b}, W.J. Dearnaley⁷¹,
 R. Debbe²⁵, C. Debenedetti⁴⁶, B. Dechenaux⁵⁵, D.V. Dedovich⁶⁴, J. Degenhardt¹²¹, J. Del Peso⁸¹,
 T. Del Prete^{123a,123b}, T. Delemontex⁵⁵, M. Deliyergiyev⁷⁴, A. Dell'Acqua³⁰, L. Dell'Asta²²,
 M. Della Pietra^{103a,i}, D. della Volpe^{103a,103b}, M. Delmastro⁵, P.A. Delsart⁵⁵, C. Deluca¹⁰⁶, S. Demers¹⁷⁷,
 M. Demichev⁶⁴, A. Demilly⁷⁹, B. Demirkoz^{12,k}, S.P. Denisov¹²⁹, D. Derendarz³⁹, J.E. Derkaoui^{136d},
 F. Derue⁷⁹, P. Dervan⁷³, K. Desch²¹, P.O. Deviveiros¹⁰⁶, A. Dewhurst¹³⁰, B. DeWilde¹⁴⁹, S. Dhaliwal¹⁰⁶,
 R. Dhullipudi^{78,l}, A. Di Ciaccio^{134a,134b}, L. Di Ciaccio⁵, C. Di Donato^{103a,103b}, A. Di Girolamo³⁰,
 B. Di Girolamo³⁰, S. Di Luise^{135a,135b}, A. Di Mattia¹⁵³, B. Di Micco^{135a,135b}, R. Di Nardo⁴⁷,
 A. Di Simone^{134a,134b}, R. Di Sipio^{20a,20b}, M.A. Diaz^{32a}, E.B. Diehl⁸⁸, J. Dietrich⁴², T.A. Dietzsch^{58a},
 S. Diglio⁸⁷, K. Dindar Yagci⁴⁰, J. Dingfelder²¹, F. Dinut^{26a}, C. Dionisi^{133a,133b}, P. Dita^{26a}, S. Dita^{26a},
 F. Dittus³⁰, F. Djama⁸⁴, T. Djobava^{51b}, M.A.B. do Vale^{24c}, A. Do Valle Wemans^{125a,m}, T.K.O. Doan⁵,
 D. Dobos³⁰, E. Dobson⁷⁷, J. Dodd³⁵, C. Doglioni⁴⁹, T. Doherty⁵³, T. Dohmae¹⁵⁶, Y. Doi^{65,*}, J. Dolejsi¹²⁸,
 Z. Dolezal¹²⁸, B.A. Dolgoshein^{97,*}, M. Donadelli^{24d}, J. Donini³⁴, J. Dopke³⁰, A. Doria^{103a},
 A. Dos Anjos¹⁷⁴, A. Dotti^{123a,123b}, M.T. Dova⁷⁰, A.T. Doyle⁵³, M. Dris¹⁰, J. Dubbert⁸⁸, S. Dube¹⁵,
 E. Dubreuil³⁴, E. Duchovni¹⁷³, G. Duckeck⁹⁹, D. Duda¹⁷⁶, A. Dudarev³⁰, F. Dudziak⁶³, L. Dufflot¹¹⁶,
 M-A. Dufour⁸⁶, L. Duguid⁷⁶, M. Dührssen³⁰, M. Dunford^{58a}, H. Duran Yildiz^{4a}, M. Düren⁵²,
 M. Dwuznik^{38a}, J. Ebke⁹⁹, S. Eckweiler⁸², W. Edson², C.A. Edwards⁷⁶, N.C. Edwards⁵³, W. Ehrenfeld²¹,
 T. Eifert¹⁴⁴, G. Eigen¹⁴, K. Einsweiler¹⁵, E. Eisenhandler⁷⁵, T. Ekelof¹⁶⁷, M. El Kacimi^{136c}, M. Ellert¹⁶⁷,
 S. Elles⁵, F. Ellinghaus⁸², K. Ellis⁷⁵, N. Ellis³⁰, J. Elmsheuser⁹⁹, M. Elsing³⁰, D. Emeliyanov¹³⁰,
 Y. Enari¹⁵⁶, O.C. Endner⁸², R. Engelmann¹⁴⁹, A. Engl⁹⁹, J. Erdmann¹⁷⁷, A. Ereditato¹⁷, D. Eriksson^{147a},
 J. Ernst², M. Ernst²⁵, J. Ernwein¹³⁷, D. Errede¹⁶⁶, S. Errede¹⁶⁶, E. Ertel⁸², M. Escalier¹¹⁶, H. Esch⁴³,
 C. Escobar¹²⁴, X. Espinal Curull¹², B. Esposito⁴⁷, F. Etienne⁸⁴, A.I. Etiennevire¹³⁷, E. Etzion¹⁵⁴,
 D. Evangelakou⁵⁴, H. Evans⁶⁰, L. Fabbri^{20a,20b}, C. Fabre³⁰, G. Facini³⁰, R.M. Fakhruddinov¹²⁹,
 S. Falciano^{133a}, Y. Fang^{33a}, M. Fanti^{90a,90b}, A. Farbin⁸, A. Farilla^{135a}, T. Farooque¹⁵⁹, S. Farrell¹⁶⁴,
 S.M. Farrington¹⁷¹, P. Farthouat³⁰, F. Fassi¹⁶⁸, P. Fassnacht³⁰, D. Fassouliotis⁹, B. Fatholahzadeh¹⁵⁹,
 A. Favareto^{90a,90b}, L. Fayard¹¹⁶, P. Federic^{145a}, O.L. Fedin¹²², W. Fedorko¹⁶⁹, M. Fehling-Kaschek⁴⁸,
 L. Feligioni⁸⁴, C. Feng^{33d}, E.J. Feng⁶, H. Feng⁸⁸, A.B. Fenyuk¹²⁹, J. Ferencei^{145b}, W. Fernando⁶,
 S. Ferrag⁵³, J. Ferrando⁵³, V. Ferrara⁴², A. Ferrari¹⁶⁷, P. Ferrari¹⁰⁶, R. Ferrari^{120a}, D.E. Ferreira de Lima⁵³,
 A. Ferrer¹⁶⁸, D. Ferrere⁴⁹, C. Ferretti⁸⁸, A. Ferretto Parodi^{50a,50b}, M. Fiassaric³¹, F. Fiedler⁸², A. Filipčič⁷⁴,
 F. Filthaut¹⁰⁵, M. Fincke-Keeler¹⁷⁰, K.D. Finelli⁴⁵, M.C.N. Fiolhais^{125a,h}, L. Fiorini¹⁶⁸, A. Firan⁴⁰,
 J. Fischer¹⁷⁶, M.J. Fisher¹¹⁰, E.A. Fitzgerald²³, M. Flechl⁴⁸, I. Fleck¹⁴², P. Fleischmann¹⁷⁵,
 S. Fleischmann¹⁷⁶, G.T. Fletcher¹⁴⁰, G. Fletcher⁷⁵, T. Flick¹⁷⁶, A. Floderus⁸⁰, L.R. Flores Castillo¹⁷⁴,
 A.C. Florez Bustos^{160b}, M.J. Flowerdew¹⁰⁰, T. Fonseca Martin¹⁷, A. Formica¹³⁷, A. Forti⁸³, D. Fortin^{160a},
 D. Fournier¹¹⁶, H. Fox⁷¹, P. Francavilla¹², M. Franchini^{20a,20b}, S. Franchino³⁰, D. Francis³⁰, M. Franklin⁵⁷,
 S. Franz³⁰, M. Fraternali^{120a,120b}, S. Fratina¹²¹, S.T. French²⁸, C. Friedrich⁴², F. Friedrich⁴⁴,
 D. Froidevaux³⁰, J.A. Frost²⁸, C. Fukunaga¹⁵⁷, E. Fullana Torregrosa¹²⁸, B.G. Fulsom¹⁴⁴, J. Fuster¹⁶⁸,
 C. Gabaldon³⁰, O. Gabizon¹⁷³, A. Gabrielli^{20a,20b}, A. Gabrielli^{133a,133b}, S. Gadatsch¹⁰⁶, T. Gadfort²⁵,
 S. Gadomski⁴⁹, G. Gagliardi^{50a,50b}, P. Gagnon⁶⁰, C. Galea⁹⁹, B. Galhardo^{125a}, E.J. Gallas¹¹⁹, V. Gallo¹⁷,
 B.J. Gallop¹³⁰, P. Gallus¹²⁷, K.K. Gan¹¹⁰, R.P. Gandrajula⁶², Y.S. Gao^{144,f}, A. Gaponenko¹⁵,
 F.M. Garay Walls⁴⁶, F. Garbersson¹⁷⁷, C. García¹⁶⁸, J.E. García Navarro¹⁶⁸, M. Garcia-Sciveres¹⁵,
 R.W. Gardner³¹, N. Garelli¹⁴⁴, V. Garonne³⁰, C. Gatti⁴⁷, G. Gaudio^{120a}, B. Gaur¹⁴², L. Gauthier⁹⁴,
 P. Gauzzi^{133a,133b}, I.L. Gavrilenko⁹⁵, C. Gay¹⁶⁹, G. Gaycken²¹, E.N. Gazis¹⁰, P. Ge^{33d,n}, Z. Gece¹⁶⁹,
 C.N.P. Gee¹³⁰, D.A.A. Geerts¹⁰⁶, Ch. Geich-Gimbel²¹, K. Gellerstedt^{147a,147b}, C. Gemme^{50a},
 A. Gemmell⁵³, M.H. Genest⁵⁵, S. Gentile^{133a,133b}, M. George⁵⁴, S. George⁷⁶, D. Gerbaudo¹⁶⁴,
 A. Gershon¹⁵⁴, H. Ghazlane^{136b}, N. Ghodbane³⁴, B. Giacobbe^{20a}, S. Giagu^{133a,133b}, V. Giangiobbe¹²,

P. Giannetti^{123a,123b}, F. Gianotti³⁰, B. Gibbard²⁵, A. Gibson¹⁵⁹, S.M. Gibson³⁰, M. Gilchriese¹⁵, T.P.S. Gillam²⁸, D. Gillberg³⁰, A.R. Gillman¹³⁰, D.M. Gingrich^{3,e}, N. Giokaris⁹, M.P. Giordani^{165c}, R. Giordano^{103a,103b}, F.M. Giorgi¹⁶, P. Giovannini¹⁰⁰, P.F. Giraud¹³⁷, D. Giugni^{90a}, C. Giuliani⁴⁸, M. Giunta⁹⁴, B.K. Gjelsten¹¹⁸, I. Gkialas^{155,o}, L.K. Gladilin⁹⁸, C. Glasman⁸¹, J. Glatzer²¹, A. Glazov⁴², G.L. Glonti⁶⁴, J.R. Goddard⁷⁵, J. Godfrey¹⁴³, J. Godlewski³⁰, M. Goebel⁴², C. Goeringer⁸², S. Goldfarb⁸⁸, T. Golling¹⁷⁷, D. Golubkov¹²⁹, A. Gomes^{125a,c}, L.S. Gomez Fajardo⁴², R. Gonçalo⁷⁶, J. Goncalves Pinto Firmino Da Costa⁴², L. Gonella²¹, S. González de la Hoz¹⁶⁸, G. Gonzalez Parra¹², M.L. Gonzalez Silva²⁷, S. Gonzalez-Sevilla⁴⁹, J.J. Goodson¹⁴⁹, L. Goossens³⁰, P.A. Gorbounov⁹⁶, H.A. Gordon²⁵, I. Gorelov¹⁰⁴, G. Gorfine¹⁷⁶, B. Gorini³⁰, E. Gorini^{72a,72b}, A. Gorišek⁷⁴, E. Gornicki³⁹, A.T. Goshaw⁶, C. Gössling⁴³, M.I. Gostkin⁶⁴, I. Gough Eschrich¹⁶⁴, M. Gouighri^{136a}, D. Goujdami^{136c}, M.P. Goulette⁴⁹, A.G. Goussiou¹³⁹, C. Goy⁵, S. Gozpinar²³, L. Graber⁵⁴, I. Grabowska-Bold^{38a}, P. Grafström^{20a,20b}, K.-J. Grahn⁴², E. Gramstad¹¹⁸, F. Grancagnolo^{72a}, S. Grancagnolo¹⁶, V. Grassi¹⁴⁹, V. Gratchev¹²², H.M. Gray³⁰, J.A. Gray¹⁴⁹, E. Graziani^{135a}, O.G. Grebenyuk¹²², T. Greenshaw⁷³, Z.D. Greenwood^{78,l}, K. Gregersen³⁶, I.M. Gregor⁴², P. Grenier¹⁴⁴, J. Griffiths⁸, N. Grigalashvili⁶⁴, A.A. Grillo¹³⁸, K. Grimm⁷¹, S. Grinstein¹², Ph. Gris³⁴, Y.V. Grishkevich⁹⁸, J.-F. Grivaz¹¹⁶, J.P. Grohs⁴⁴, A. Grohsjean⁴², E. Gross¹⁷³, J. Grosse-Knetter⁵⁴, J. Groth-Jensen¹⁷³, K. Grybel¹⁴², F. Guescini⁴⁹, D. Guest¹⁷⁷, O. Gueta¹⁵⁴, C. Guicheney³⁴, E. Guido^{50a,50b}, T. Guillemin¹¹⁶, S. Guindon², U. Gul⁵³, J. Gunther¹²⁷, J. Guo³⁵, P. Gutierrez¹¹², N. Guttman¹⁵⁴, O. Gutzwiller¹⁷⁴, C. Guyot¹³⁷, C. Gwenlan¹¹⁹, C.B. Gwilliam⁷³, A. Haas¹⁰⁹, S. Haas³⁰, C. Haber¹⁵, H.K. Hadavand⁸, P. Haefner²¹, Z. Hajduk³⁹, H. Hakobyan¹⁷⁸, D. Hall¹¹⁹, G. Halladjian⁶², K. Hamacher¹⁷⁶, P. Hamal¹¹⁴, K. Hamano⁸⁷, M. Hamer⁵⁴, A. Hamilton^{146a,p}, S. Hamilton¹⁶², L. Han^{33b}, K. Hanagaki¹¹⁷, K. Hanawa¹⁶¹, M. Hance¹⁵, C. Handel⁸², P. Hanke^{58a}, J.R. Hansen³⁶, J.B. Hansen³⁶, J.D. Hansen³⁶, P.H. Hansen³⁶, P. Hansson¹⁴⁴, K. Hara¹⁶¹, A.S. Hard¹⁷⁴, T. Harenberg¹⁷⁶, S. Harkusha⁹¹, D. Harper⁸⁸, R.D. Harrington⁴⁶, O.M. Harris¹³⁹, J. Hartert⁴⁸, F. Hartjes¹⁰⁶, T. Haruyama⁶⁵, A. Harvey⁵⁶, S. Hasegawa¹⁰², Y. Hasegawa¹⁴¹, S. Hassani¹³⁷, S. Haug¹⁷, M. Hauschild³⁰, R. Hauser⁸⁹, M. Havranek²¹, C.M. Hawkes¹⁸, R.J. Hawkins³⁰, A.D. Hawkins⁸⁰, T. Hayakawa⁶⁶, T. Hayashi¹⁶¹, D. Hayden⁷⁶, C.P. Hays¹¹⁹, H.S. Hayward⁷³, S.J. Haywood¹³⁰, S.J. Head¹⁸, T. Heck⁸², V. Hedberg⁸⁰, L. Heelan⁸, S. Heim¹²¹, B. Heinemann¹⁵, S. Heisterkamp³⁶, J. Hejbal¹²⁶, L. Helary²², C. Heller⁹⁹, M. Heller³⁰, S. Hellman^{147a,147b}, D. Hellmich²¹, C. Helsen³⁰, J. Henderson¹¹⁹, R.C.W. Henderson⁷¹, M. Henke^{58a}, A. Henrichs¹⁷⁷, A.M. Henriques Correia³⁰, S. Henrot-Versille¹¹⁶, C. Hensel⁵⁴, G.H. Herbert¹⁶, C.M. Hernandez⁸, Y. Hernández Jiménez¹⁶⁸, R. Herrberg-Schubert¹⁶, G. Herten⁴⁸, R. Hertenberger⁹⁹, L. Hervas³⁰, G.G. Hesketh⁷⁷, N.P. Hessey¹⁰⁶, R. Hickling⁷⁵, E. Higón-Rodríguez¹⁶⁸, J.C. Hill²⁸, K.H. Hiller⁴², S. Hillert²¹, S.J. Hillier¹⁸, I. Hinchliffe¹⁵, E. Hines¹²¹, M. Hirose¹¹⁷, D. Hirschebuehl¹⁷⁶, J. Hobbs¹⁴⁹, N. Hod¹⁰⁶, M.C. Hodgkinson¹⁴⁰, P. Hodgson¹⁴⁰, A. Hoecker³⁰, M.R. Hoferkamp¹⁰⁴, J. Hoffman⁴⁰, D. Hoffmann⁸⁴, J.I. Hofmann^{58a}, M. Hohlfeld⁸², S.O. Holmgren^{147a}, J.L. Holzbauer⁸⁹, T.M. Hong¹²¹, L. Hooft van Huysduynen¹⁰⁹, J.-Y. Hostachy⁵⁵, S. Hou¹⁵², A. Hoummada^{136a}, J. Howard¹¹⁹, J. Howarth⁸³, M. Hrabovsky¹¹⁴, I. Hristova¹⁶, J. Hrivnac¹¹⁶, T. Hryn'ova⁵, P.J. Hsu⁸², S.-C. Hsu¹³⁹, D. Hu³⁵, X. Hu²⁵, Z. Hubacek³⁰, F. Hubaut⁸⁴, F. Huegging²¹, A. Huettmann⁴², T.B. Huffman¹¹⁹, E.W. Hughes³⁵, G. Hughes⁷¹, M. Huhtinen³⁰, T.A. Hülsing⁸², M. Hurwitz¹⁵, N. Huseynov^{64,q}, J. Huston⁸⁹, J. Huth⁵⁷, G. Iacobucci⁴⁹, G. Iakovidis¹⁰, I. Ibragimov¹⁴², L. Iconomidou-Fayard¹¹⁶, J. Idarraga¹¹⁶, P. Iengo^{103a}, O. Igonkina¹⁰⁶, Y. Ikegami⁶⁵, K. Ikematsu¹⁴², M. Ikeno⁶⁵, D. Iliadis¹⁵⁵, N. Ilic¹⁵⁹, T. Ince¹⁰⁰, P. Ioannou⁹, M. Iodice^{135a}, K. Iordanidou⁹, V. Ippolito^{133a,133b}, A. Irlès Quiles¹⁶⁸, C. Isaksson¹⁶⁷, M. Ishino⁶⁷, M. Ishitsuka¹⁵⁸, R. Ishmukhametov¹¹⁰, C. Issever¹¹⁹, S. Istin^{19a}, A.V. Ivashin¹²⁹, W. Iwanski³⁹, H. Iwasaki⁶⁵, J.M. Izen⁴¹, V. Izzo^{103a}, B. Jackson¹²¹, J.N. Jackson⁷³, P. Jackson¹, M.R. Jaekel³⁰, V. Jain², K. Jakobs⁴⁸, S. Jakobsen³⁶, T. Jakoubek¹²⁶, J. Jakubek¹²⁷, D.O. Jamin¹⁵², D.K. Jana¹¹², E. Jansen⁷⁷, H. Jansen³⁰, J. Janssen²¹, A. Jantsch¹⁰⁰, M. Janus⁴⁸, R.C. Jared¹⁷⁴, G. Jarlskog⁸⁰, L. Jeanty⁵⁷, G.-Y. Jeng¹⁵¹, I. Jen-La Plante³¹, D. Jennens⁸⁷, P. Jenni³⁰, J. Jentsch⁴³, C. Jeske¹⁷¹, P. Jež³⁶, S. Jézéquel⁵, M.K. Jha^{20a}, H. Ji¹⁷⁴, W. Ji⁸², J. Jia¹⁴⁹, Y. Jiang^{33b}, M. Jimenez Belenguer⁴², S. Jin^{33a}, O. Jinnouchi¹⁵⁸, M.D. Joergensen³⁶, D. Joffe⁴⁰,

M. Johansen^{147a,147b}, K.E. Johansson^{147a}, P. Johansson¹⁴⁰, S. Johnert⁴², K.A. Johns⁷, K. Jon-And^{147a,147b}, G. Jones¹⁷¹, R.W.L. Jones⁷¹, T.J. Jones⁷³, P.M. Jorge^{125a}, K.D. Joshi⁸³, J. Jovicevic¹⁴⁸, T. Jovin^{13b}, X. Ju¹⁷⁴, C.A. Jung⁴³, R.M. Jungst³⁰, P. Jussel⁶¹, A. Juste Rozas¹², S. Kabana¹⁷, M. Kaci¹⁶⁸, A. Kaczmarek³⁹, P. Kadlecik³⁶, M. Kado¹¹⁶, H. Kagan¹¹⁰, M. Kagan⁵⁷, E. Kajomovitz¹⁵³, S. Kalinin¹⁷⁶, S. Kama⁴⁰, N. Kanaya¹⁵⁶, M. Kaneda³⁰, S. Kaneti²⁸, T. Kanno¹⁵⁸, V.A. Kantserov⁹⁷, J. Kanzaki⁶⁵, B. Kaplan¹⁰⁹, A. Kapliy³¹, D. Kar⁵³, K. Karakostas¹⁰, M. Karnevskiy⁸², V. Kartvelishvili⁷¹, A.N. Karyukhin¹²⁹, L. Kashif¹⁷⁴, G. Kasieczka^{58b}, R.D. Kass¹¹⁰, A. Kastanas¹⁴, Y. Kataoka¹⁵⁶, J. Katzy⁴², V. Kaushik⁷, K. Kawagoe⁶⁹, T. Kawamoto¹⁵⁶, G. Kawamura⁵⁴, S. Kazama¹⁵⁶, V.F. Kazanin¹⁰⁸, M.Y. Kazarinov⁶⁴, R. Keeler¹⁷⁰, P.T. Keener¹²¹, R. Kehoe⁴⁰, M. Keil⁵⁴, J.S. Keller¹³⁹, H. Keoshkerian⁵, O. Kepka¹²⁶, B.P. Kerševan⁷⁴, S. Kersten¹⁷⁶, K. Kessoku¹⁵⁶, J. Keung¹⁵⁹, F. Khalil-zada¹¹, H. Khandanyan^{147a,147b}, A. Khanov¹¹³, D. Kharchenko⁶⁴, A. Khodinov⁹⁷, A. Khomich^{58a}, T.J. Khoo²⁸, G. Khorauli²¹, A. Khoroshilov¹⁷⁶, V. Khovanskiy⁹⁶, E. Khramov⁶⁴, J. Khubua^{51b}, H. Kim^{147a,147b}, S.H. Kim¹⁶¹, N. Kimura¹⁷², O. Kind¹⁶, B.T. King⁷³, M. King⁶⁶, R.S.B. King¹¹⁹, S.B. King¹⁶⁹, J. Kirk¹³⁰, A.E. Kiryunin¹⁰⁰, T. Kishimoto⁶⁶, D. Kisielewska^{38a}, T. Kitamura⁶⁶, T. Kittelmann¹²⁴, K. Kiuchi¹⁶¹, E. Kladiva^{145b}, M. Klein⁷³, U. Klein⁷³, K. Kleinknecht⁸², M. Klemetti⁸⁶, A. Klier¹⁷³, P. Klimek^{147a,147b}, A. Klimentov²⁵, R. Klingenberg⁴³, J.A. Klinger⁸³, E.B. Klinkby³⁶, T. Klioutchnikova³⁰, P.F. Klok¹⁰⁵, E.-E. Kluge^{58a}, P. Kluit¹⁰⁶, S. Kluth¹⁰⁰, E. Kneringer⁶¹, E.B.F.G. Knoops⁸⁴, A. Knue⁵⁴, B.R. Ko⁴⁵, T. Kobayashi¹⁵⁶, M. Kobel⁴⁴, M. Kocian¹⁴⁴, P. Kodys¹²⁸, S. Koenig⁸², F. Koetsveld¹⁰⁵, P. Koevesarki²¹, T. Koffas²⁹, E. Koffeman¹⁰⁶, L.A. Kogan¹¹⁹, S. Kohlmann¹⁷⁶, F. Kohn⁵⁴, Z. Kohout¹²⁷, T. Kohriki⁶⁵, T. Koi¹⁴⁴, H. Kolanoski¹⁶, I. Koletsou^{90a}, J. Koll⁸⁹, A.A. Komar⁹⁵, Y. Komori¹⁵⁶, T. Kondo⁶⁵, K. Köneke³⁰, A.C. König¹⁰⁵, T. Kono^{42,r}, A.I. Kononov⁴⁸, R. Konoplich^{109,s}, N. Konstantinidis⁷⁷, R. Kopeliansky¹⁵³, S. Koperny^{38a}, L. Köpke⁸², A.K. Kopp⁴⁸, K. Korcyl³⁹, K. Kordas¹⁵⁵, A. Korn⁴⁶, A. Korol¹⁰⁸, I. Korolkov¹², E.V. Korolkova¹⁴⁰, V.A. Korotkov¹²⁹, O. Kortner¹⁰⁰, S. Kortner¹⁰⁰, V.V. Kostyukhin²¹, S. Kotov¹⁰⁰, V.M. Kotov⁶⁴, A. Kotwal⁴⁵, C. Kourkoumelis⁹, V. Kouskoura¹⁵⁵, A. Koutsman^{160a}, R. Kowalewski¹⁷⁰, T.Z. Kowalski^{38a}, W. Kozanecki¹³⁷, A.S. Kozhin¹²⁹, V. Kral¹²⁷, V.A. Kramarenko⁹⁸, G. Kramberger⁷⁴, M.W. Krasny⁷⁹, A. Krasznahorkay¹⁰⁹, J.K. Kraus²¹, A. Kravchenko²⁵, S. Kreiss¹⁰⁹, J. Kretschmar⁷³, K. Kreutzfeldt⁵², N. Krieger⁵⁴, P. Krieger¹⁵⁹, K. Kroeninger⁵⁴, H. Kroha¹⁰⁰, J. Kroll¹²¹, J. Kroseberg²¹, J. Krstic^{13a}, U. Kruchonak⁶⁴, H. Krüger²¹, T. Kruker¹⁷, N. Krumnack⁶³, Z.V. Krumshteyn⁶⁴, A. Kruse¹⁷⁴, M.K. Kruse⁴⁵, M. Kruskal²², T. Kubota⁸⁷, S. Kuday^{4a}, S. Kuehn⁴⁸, A. Kugel^{58c}, T. Kuhl⁴², V. Kukhtin⁶⁴, Y. Kulchitsky⁹¹, S. Kuleshov^{32b}, M. Kuna⁷⁹, J. Kunkle¹²¹, A. Kupco¹²⁶, H. Kurashige⁶⁶, M. Kurata¹⁶¹, Y.A. Kurochkin⁹¹, V. Kus¹²⁶, E.S. Kuwertz¹⁴⁸, M. Kuze¹⁵⁸, J. Kvita¹⁴³, R. Kwee¹⁶, A. La Rosa⁴⁹, L. La Rotonda^{37a,37b}, L. Labarga⁸¹, S. Lablak^{136a}, C. Lacasta¹⁶⁸, F. Lacava^{133a,133b}, J. Lacey²⁹, H. Lacker¹⁶, D. Lacour⁷⁹, V.R. Lacuesta¹⁶⁸, E. Ladygin⁶⁴, R. Lafaye⁵, B. Laforge⁷⁹, T. Lagouri¹⁷⁷, S. Lai⁴⁸, H. Laier^{58a}, E. Laisne⁵⁵, L. Lambourne⁷⁷, C.L. Lampen⁷, W. Lampl⁷, E. Lançon¹³⁷, U. Landgraf⁴⁸, M.P.J. Landon⁷⁵, V.S. Lang^{58a}, C. Lange⁴², A.J. Lankford¹⁶⁴, F. Lanni²⁵, K. Lantzsck³⁰, A. Lanza^{120a}, S. Laplace⁷⁹, C. Lapoire²¹, J.F. Laporte¹³⁷, T. Lari^{90a}, A. Larner¹¹⁹, M. Lassnig³⁰, P. Laurelli⁴⁷, V. Lavorini^{37a,37b}, W. Lavrijsen¹⁵, P. Laycock⁷³, O. Le Dortz⁷⁹, E. Le Guirriec⁸⁴, E. Le Menedeu¹², T. LeCompte⁶, F. Ledroit-Guillon⁵⁵, H. Lee¹⁰⁶, J.S.H. Lee¹¹⁷, S.C. Lee¹⁵², L. Lee¹⁷⁷, G. Lefebvre⁷⁹, M. Lefebvre¹⁷⁰, M. Legendre¹³⁷, F. Legger⁹⁹, C. Leggett¹⁵, M. Lehmacher²¹, G. Lehmann Miotto³⁰, A.G. Leister¹⁷⁷, M.A.L. Leite^{24d}, R. Leitner¹²⁸, D. Lellouch¹⁷³, B. Lemmer⁵⁴, V. Lendermann^{58a}, K.J.C. Leney^{146c}, T. Lenz¹⁰⁶, G. Lenzen¹⁷⁶, B. Lenzi³⁰, K. Leonhardt⁴⁴, S. Leontsinis¹⁰, F. Lepold^{58a}, C. Leroy⁹⁴, J.-R. Lessard¹⁷⁰, C.G. Lester²⁸, C.M. Lester¹²¹, J. Levêque⁵, D. Levin⁸⁸, L.J. Levinson¹⁷³, A. Lewis¹¹⁹, G.H. Lewis¹⁰⁹, A.M. Leyko²¹, M. Leyton¹⁶, B. Li^{33b}, B. Li⁸⁴, H. Li¹⁴⁹, H.L. Li³¹, S. Li^{33b,t}, X. Li⁸⁸, Z. Liang^{119,u}, H. Liao³⁴, B. Liberti^{134a}, P. Lichard³⁰, K. Lie¹⁶⁶, J. Liebal²¹, W. Liebig¹⁴, C. Limbach²¹, A. Limosani⁸⁷, M. Limper⁶², S.C. Lin^{152,v}, F. Linde¹⁰⁶, B.E. Lindquist¹⁴⁹, J.T. Linnemann⁸⁹, E. Lipeles¹²¹, A. Lipniacka¹⁴, M. Lisovsky⁴², T.M. Liss¹⁶⁶, D. Lissauer²⁵, A. Lister¹⁶⁹, A.M. Litke¹³⁸, D. Liu¹⁵², J.B. Liu^{33b}, K. Liu^{33b,w}, L. Liu⁸⁸, M. Liu⁴⁵, M. Liu^{33b}, Y. Liu^{33b}, M. Livan^{120a,120b}, S.S.A. Livermore¹¹⁹, A. Lleres⁵⁵, J. Llorente Merino⁸¹, S.L. Lloyd⁷⁵, F. Lo Sterzo^{133a,133b}, E. Lobodzinska⁴², P. Loch⁷,

W.S. Lockman¹³⁸, T. Loddenkoetter²¹, F.K. Loebinger⁸³, A.E. Loevschall-Jensen³⁶, A. Loginov¹⁷⁷, C.W. Loh¹⁶⁹, T. Lohse¹⁶, K. Lohwasser⁴⁸, M. Lokajicek¹²⁶, V.P. Lombardo⁵, R.E. Long⁷¹, L. Lopes^{125a}, D. Lopez Mateos⁵⁷, J. Lorenz⁹⁹, N. Lorenzo Martinez¹¹⁶, M. Losada¹⁶³, P. Loscutoff¹⁵, M.J. Losty^{160a,*}, X. Lou⁴¹, A. Lounis¹¹⁶, K.F. Loureiro¹⁶³, J. Love⁶, P.A. Love⁷¹, A.J. Lowe^{144.f}, F. Lu^{33a}, H.J. Lubatti¹³⁹, C. Luci^{133a,133b}, A. Lucotte⁵⁵, D. Ludwig⁴², I. Ludwig⁴⁸, J. Ludwig⁴⁸, F. Luehring⁶⁰, W. Lukas⁶¹, L. Luminari^{133a}, E. Lund¹¹⁸, J. Lundberg^{147a,147b}, O. Lundberg^{147a,147b}, B. Lund-Jensen¹⁴⁸, J. Lundquist³⁶, M. Lungwitz⁸², D. Lynn²⁵, R. Lysak¹²⁶, E. Lytken⁸⁰, H. Ma²⁵, L.L. Ma¹⁷⁴, G. Maccarrone⁴⁷, A. Macchiolo¹⁰⁰, B. Maček⁷⁴, J. Machado Miguens^{125a}, D. Macina³⁰, R. Mackeprang³⁶, R. Madar⁴⁸, R.J. Madaras¹⁵, H.J. Maddocks⁷¹, W.F. Mader⁴⁴, A. Madsen¹⁶⁷, M. Maeno⁵, T. Maeno²⁵, L. Magnoni¹⁶⁴, E. Magradze⁵⁴, K. Mahboubi⁴⁸, J. Mahlstedt¹⁰⁶, S. Mahmoud⁷³, G. Mahout¹⁸, C. Maiani¹³⁷, C. Maidantchik^{24a}, A. Maio^{125a,c}, S. Majewski¹¹⁵, Y. Makida⁶⁵, N. Makovec¹¹⁶, P. Mal^{137,x}, B. Malaescu⁷⁹, Pa. Malecki³⁹, P. Malecki³⁹, V.P. Maleev¹²², F. Malek⁵⁵, U. Mallik⁶², D. Malon⁶, C. Malone¹⁴⁴, S. Maltezos¹⁰, V. Malyshev¹⁰⁸, S. Malyukov³⁰, J. Mamuzic^{13b}, L. Mandelli^{90a}, I. Mandić⁷⁴, R. Mandrysch⁶², J. Maneira^{125a}, A. Manfredini¹⁰⁰, L. Manhaes de Andrade Filho^{24b}, J.A. Manjarres Ramos¹³⁷, A. Mann⁹⁹, P.M. Manning¹³⁸, A. Manousakis-Katsikakis⁹, B. Mansoulie¹³⁷, R. Mantifel⁸⁶, L. Mapelli³⁰, L. March¹⁶⁸, J.F. Marchand²⁹, F. Marchese^{134a,134b}, G. Marchiori⁷⁹, M. Marcisovsky¹²⁶, C.P. Marino¹⁷⁰, C.N. Marques^{125a}, F. Marroquim^{24a}, Z. Marshall¹²¹, L.F. Marti¹⁷, S. Marti-Garcia¹⁶⁸, B. Martin³⁰, B. Martin⁸⁹, J.P. Martin⁹⁴, T.A. Martin¹⁷¹, V.J. Martin⁴⁶, B. Martin dit Latour⁴⁹, H. Martinez¹³⁷, M. Martinez¹², S. Martin-Haugh¹⁵⁰, A.C. Martyniuk¹⁷⁰, M. Marx⁸³, F. Marzano^{133a}, A. Marzin¹¹², L. Masetti⁸², T. Mashimo¹⁵⁶, R. Mashinistov⁹⁵, J. Masik⁸³, A.L. Maslennikov¹⁰⁸, I. Massa^{20a,20b}, N. Massol⁵, P. Mastrandrea¹⁴⁹, A. Mastroberardino^{37a,37b}, T. Masubuchi¹⁵⁶, H. Matsunaga¹⁵⁶, T. Matsushita⁶⁶, P. Mättig¹⁷⁶, S. Mättig⁴², C. Mattraversi^{119,d}, J. Maurer⁸⁴, S.J. Maxfield⁷³, D.A. Maximov^{108,g}, R. Mazini¹⁵², M. Mazur²¹, L. Mazzaferro^{134a,134b}, M. Mazzanti^{90a}, S.P. Mc Kee⁸⁸, A. McCarn¹⁶⁶, R.L. McCarthy¹⁴⁹, T.G. McCarthy²⁹, N.A. McCubbin¹³⁰, K.W. McFarlane^{56,*}, J.A. McFayden¹⁴⁰, G. Mchedlidze^{51b}, T. McLaughlan¹⁸, S.J. McMahon¹³⁰, R.A. McPherson^{170,j}, A. Meade⁸⁵, J. Mechnich¹⁰⁶, M. Mechtel¹⁷⁶, M. Medinnis⁴², S. Meehan³¹, R. Meera-Lebbai¹¹², T. Meguro¹¹⁷, S. Mehlhase³⁶, A. Mehta⁷³, K. Meier^{58a}, C. Meineck⁹⁹, B. Meirose⁸⁰, C. Melachrinos³¹, B.R. Mellado Garcia^{146c}, F. Meloni^{90a,90b}, L. Mendoza Navas¹⁶³, A. Mengarelli^{20a,20b}, S. Menke¹⁰⁰, E. Meoni¹⁶², K.M. Mercurio⁵⁷, N. Meric¹³⁷, P. Mermod⁴⁹, L. Merola^{103a,103b}, C. Meroni^{90a}, F.S. Merritt³¹, H. Merritt¹¹⁰, A. Messina^{30,y}, J. Metcalfe²⁵, A.S. Mete¹⁶⁴, C. Meyer⁸², C. Meyer³¹, J-P. Meyer¹³⁷, J. Meyer³⁰, J. Meyer⁵⁴, S. Michal³⁰, R.P. Middleton¹³⁰, S. Migas⁷³, L. Mijović¹³⁷, G. Mikenberg¹⁷³, M. Mikestikova¹²⁶, M. Mikuž⁷⁴, D.W. Miller³¹, W.J. Mills¹⁶⁹, C. Mills⁵⁷, A. Milov¹⁷³, D.A. Milstead^{147a,147b}, D. Milstein¹⁷³, A.A. Minaenko¹²⁹, M. Miñano Moya¹⁶⁸, I.A. Minashvili⁶⁴, A.I. Mincer¹⁰⁹, B. Mindur^{38a}, M. Mineev⁶⁴, Y. Ming¹⁷⁴, L.M. Mir¹², G. Mirabelli^{133a}, J. Mitrevski¹³⁸, V.A. Mitsou¹⁶⁸, S. Mitsui⁶⁵, P.S. Miyagawa¹⁴⁰, J.U. Mjörnmark⁸⁰, T. Moe^{147a,147b}, V. Moeller²⁸, S. Mohapatra¹⁴⁹, W. Mohr⁴⁸, R. Moles-Valls¹⁶⁸, A. Molfetas³⁰, K. Mönig⁴², C. Monini⁵⁵, J. Monk³⁶, E. Monnier⁸⁴, J. Montejo Berlingen¹², F. Monticelli⁷⁰, S. Monzani^{20a,20b}, R.W. Moore³, C. Mora Herrera⁴⁹, A. Moraes⁵³, N. Morange⁶², J. Morel⁵⁴, D. Moreno⁸², M. Moreno Llácer¹⁶⁸, P. Morettini^{50a}, M. Morgenstern⁴⁴, M. Morii⁵⁷, S. Moritz⁸², A.K. Morley³⁰, G. Mornacchi³⁰, J.D. Morris⁷⁵, L. Morvaj¹⁰², N. Möser²¹, H.G. Moser¹⁰⁰, M. Mosidze^{51b}, J. Moss¹¹⁰, R. Mount¹⁴⁴, E. Mountricha^{10,z}, S.V. Mouraviev^{95,*}, E.J.W. Moyses⁸⁵, R.D. Mudd¹⁸, F. Mueller^{58a}, J. Mueller¹²⁴, K. Mueller²¹, T. Mueller²⁸, T. Mueller⁸², D. Muenstermann³⁰, Y. Munwes¹⁵⁴, J.A. Murillo Quijada¹⁸, W.J. Murray¹³⁰, I. Mussche¹⁰⁶, E. Musto¹⁵³, A.G. Myagkov^{129,aa}, M. Myska¹²⁶, O. Nackenhurst⁵⁴, J. Nadal¹², K. Nagai¹⁶¹, R. Nagai¹⁵⁸, Y. Nagai⁸⁴, K. Nagano⁶⁵, A. Nagarkar¹¹⁰, Y. Nagasaka⁵⁹, M. Nagel¹⁰⁰, A.M. Nairz³⁰, Y. Nakahama³⁰, K. Nakamura⁶⁵, T. Nakamura¹⁵⁶, I. Nakano¹¹¹, H. Namasivayam⁴¹, G. Nanava²¹, A. Napier¹⁶², R. Narayan^{58b}, M. Nash^{77,d}, T. Nattermann²¹, T. Naumann⁴², G. Navarro¹⁶³, H.A. Neal⁸⁸, P.Yu. Nechaeva⁹⁵, T.J. Neep⁸³, A. Negri^{120a,120b}, G. Negri³⁰, M. Negrini^{20a}, S. Nektarijevic⁴⁹, A. Nelson¹⁶⁴, T.K. Nelson¹⁴⁴, S. Nemecek¹²⁶, P. Nemethy¹⁰⁹, A.A. Nepomuceno^{24a}, M. Nessi^{30,ab}, M.S. Neubauer¹⁶⁶,

M. Neumann¹⁷⁶, A. Neusiedl⁸², R.M. Neves¹⁰⁹, P. Nevski²⁵, F.M. Newcomer¹²¹, P.R. Newman¹⁸, D.H. Nguyen⁶, V. Nguyen Thi Hong¹³⁷, R.B. Nickerson¹¹⁹, R. Nicolaidou¹³⁷, B. Nicquevert³⁰, F. Niedercorn¹¹⁶, J. Nielsen¹³⁸, N. Nikiforou³⁵, A. Nikiforov¹⁶, V. Nikolaenko^{129,aa}, I. Nikolic-Audit⁷⁹, K. Nikolics⁴⁹, K. Nikolopoulos¹⁸, P. Nilsson⁸, Y. Ninomiya¹⁵⁶, A. Nisati^{133a}, R. Nisius¹⁰⁰, T. Nobe¹⁵⁸, L. Nodulman⁶, M. Nomachi¹¹⁷, I. Nomidis¹⁵⁵, S. Norberg¹¹², M. Nordberg³⁰, J. Novakova¹²⁸, M. Nozaki⁶⁵, L. Nozka¹¹⁴, A.-E. Nuncio-Quiroz²¹, G. Nunes Hanninger⁸⁷, T. Nunnemann⁹⁹, E. Nurse⁷⁷, B.J. O'Brien⁴⁶, D.C. O'Neil¹⁴³, V. O'Shea⁵³, L.B. Oakes⁹⁹, F.G. Oakham^{29,e}, H. Oberlack¹⁰⁰, J. Ocariz⁷⁹, A. Ochi⁶⁶, M.I. Ochoa⁷⁷, S. Oda⁶⁹, S. Odaka⁶⁵, J. Odier⁸⁴, H. Ogren⁶⁰, A. Oh⁸³, S.H. Oh⁴⁵, C.C. Ohm³⁰, T. Ohshima¹⁰², W. Okamura¹¹⁷, H. Okawa²⁵, Y. Okumura³¹, T. Okuyama¹⁵⁶, A. Olariu^{26a}, A.G. Olchevski⁶⁴, S.A. Olivares Pino⁴⁶, M. Oliveira^{125a,h}, D. Oliveira Damazio²⁵, E. Oliver Garcia¹⁶⁸, D. Olivito¹²¹, A. Olszewski³⁹, J. Olszowska³⁹, A. Onofre^{125a,ac}, P.U.E. Onyisi^{31,ad}, C.J. Oram^{160a}, M.J. Oreglia³¹, Y. Oren¹⁵⁴, D. Orestano^{135a,135b}, N. Orlando^{72a,72b}, C. Oropeza Barrera⁵³, R.S. Orr¹⁵⁹, B. Osculati^{50a,50b}, R. Ospanov¹²¹, G. Otero y Garzon²⁷, J.P. Ottersbach¹⁰⁶, M. Ouchrif^{136d}, E.A. Ouellette¹⁷⁰, F. Ould-Saada¹¹⁸, A. Ouraou¹³⁷, Q. Ouyang^{33a}, A. Ovcharova¹⁵, M. Owen⁸³, S. Owen¹⁴⁰, V.E. Ozcan^{19a}, N. Ozturk⁸, A. Pacheco Pages¹², C. Padilla Aranda¹², S. Pagan Griso¹⁵, E. Paganis¹⁴⁰, C. Pahl¹⁰⁰, F. Paige²⁵, P. Pais⁸⁵, K. Pajchel¹¹⁸, G. Palacino^{160b}, C.P. Paleari⁷, S. Palestini³⁰, D. Pallin³⁴, A. Palma^{125a}, J.D. Palmer¹⁸, Y.B. Pan¹⁷⁴, E. Panagiotopoulou¹⁰, J.G. Panduro Vazquez⁷⁶, P. Pani¹⁰⁶, N. Panikashvili⁸⁸, S. Panitkin²⁵, D. Pantea^{26a}, A. Papadelis^{147a}, Th.D. Papadopoulou¹⁰, K. Papageorgiou^{155,o}, A. Paramonov⁶, D. Paredes Hernandez³⁴, W. Park^{25,ae}, M.A. Parker²⁸, F. Parodi^{50a,50b}, J.A. Parsons³⁵, U. Parzefall⁴⁸, S. Pashapour⁵⁴, E. Pasqualucci^{133a}, S. Passaggio^{50a}, A. Passeri^{135a}, F. Pastore^{135a,135b,*}, Fr. Pastore⁷⁶, G. Pásztor^{49,af}, S. Patarraia¹⁷⁶, N.D. Patel¹⁵¹, J.R. Pater⁸³, S. Patricelli^{103a,103b}, T. Pauly³⁰, J. Pearce¹⁷⁰, M. Pedersen¹¹⁸, S. Pedraza Lopez¹⁶⁸, M.I. Pedraza Morales¹⁷⁴, S.V. Peleganchuk¹⁰⁸, D. Pelikan¹⁶⁷, H. Peng^{33b}, B. Penning³¹, A. Penson³⁵, J. Penwell⁶⁰, T. Perez Cavalcanti⁴², E. Perez Codina^{160a}, M.T. Pérez García-Estañ¹⁶⁸, V. Perez Reale³⁵, L. Perini^{90a,90b}, H. Pernegger³⁰, R. Perrino^{72a}, P. Perrodo⁵, V.D. Peshekhonov⁶⁴, K. Peters³⁰, R.F.Y. Peters^{54,ag}, B.A. Petersen³⁰, J. Petersen³⁰, T.C. Petersen³⁶, E. Petit⁵, A. Petridis^{147a,147b}, C. Petridou¹⁵⁵, E. Petrolo^{133a}, F. Petrucci^{135a,135b}, D. Petschull⁴², M. Petteni¹⁴³, R. Pezoa^{32b}, A. Phan⁸⁷, P.W. Phillips¹³⁰, G. Piacquadio¹⁴⁴, E. Pianori¹⁷¹, A. Picazio⁴⁹, E. Piccaro⁷⁵, M. Piccinini^{20a,20b}, S.M. Piec⁴², R. Piegai²⁷, D.T. Pignotti¹¹⁰, J.E. Pilcher³¹, A.D. Pilkington⁸³, J. Pina^{125a,c}, M. Pinamonti^{165a,165c,ah}, A. Pinder¹¹⁹, J.L. Pinfold³, A. Pingel³⁶, B. Pinto^{125a}, C. Pizio^{90a,90b}, M.-A. Pleier²⁵, V. Pleskot¹²⁸, E. Plotnikova⁶⁴, P. Plucinski^{147a,147b}, S. Poddar^{58a}, F. Podlyski³⁴, R. Poettgen⁸², L. Poggioli¹¹⁶, D. Pohl²¹, M. Pohl⁴⁹, G. Polesello^{120a}, A. Policicchio^{37a,37b}, R. Polifka¹⁵⁹, A. Polini^{20a}, V. Polychronakos²⁵, D. Pomeroy²³, K. Pommès³⁰, L. Pontecorvo^{133a}, B.G. Pope⁸⁹, G.A. Popeneciu^{26b}, D.S. Popovic^{13a}, A. Poppleton³⁰, X. Portell Bueso¹², G.E. Pospelov¹⁰⁰, S. Pospisil¹²⁷, I.N. Potrap⁶⁴, C.J. Potter¹⁵⁰, C.T. Potter¹¹⁵, G. Poulard³⁰, J. Poveda⁶⁰, V. Pozdnyakov⁶⁴, R. Prabhu⁷⁷, P. Pralavorio⁸⁴, A. Pranko¹⁵, S. Prasad³⁰, R. Pravahan²⁵, S. Prell⁶³, K. Pretzl¹⁷, D. Price⁶⁰, J. Price⁷³, L.E. Price⁶, D. Prieur¹²⁴, M. Primavera^{72a}, M. Proissl⁴⁶, K. Prokofiev¹⁰⁹, F. Prokoshin^{32b}, E. Protopapadaki¹³⁷, S. Protopopescu²⁵, J. Proudfoot⁶, X. Prudent⁴⁴, M. Przybycien^{38a}, H. Przysiezniak⁵, S. Psoroulas²¹, E. Ptacek¹¹⁵, E. Pueschel⁸⁵, D. Puldon¹⁴⁹, M. Purohit^{25,ae}, P. Puzo¹¹⁶, Y. Pylypchenko⁶², J. Qian⁸⁸, A. Quad⁵⁴, D.R. Quarrie¹⁵, W.B. Quayle¹⁷⁴, D. Quilty⁵³, M. Raas¹⁰⁵, V. Radeka²⁵, V. Radescu⁴², P. Radloff¹¹⁵, F. Ragusa^{90a,90b}, G. Rahal¹⁷⁹, S. Rajagopalan²⁵, M. Rammensee⁴⁸, M. Rammes¹⁴², A.S. Randle-Conde⁴⁰, K. Randrianarivony²⁹, C. Rangel-Smith⁷⁹, K. Rao¹⁶⁴, F. Rauscher⁹⁹, T.C. Rave⁴⁸, T. Ravenscroft⁵³, M. Raymond³⁰, A.L. Read¹¹⁸, D.M. Rebuszi^{120a,120b}, A. Redelbach¹⁷⁵, G. Redlinger²⁵, R. Reece¹²¹, K. Reeves⁴¹, A. Reinsch¹¹⁵, I. Reisinger⁴³, M. Relich¹⁶⁴, C. Rembser³⁰, Z.L. Ren¹⁵², A. Renaud¹¹⁶, M. Rescigno^{133a}, S. Resconi^{90a}, B. Resende¹³⁷, P. Reznicek⁹⁹, R. Rezvani⁹⁴, R. Richter¹⁰⁰, E. Richter-Was^{38b}, M. Ridel⁷⁹, P. Rieck¹⁶, M. Rijssenbeek¹⁴⁹, A. Rimoldi^{120a,120b}, L. Rinaldi^{20a}, R.R. Rios⁴⁰, E. Ritsch⁶¹, I. Riu¹², G. Rivoltella^{90a,90b}, F. Rizatdinova¹¹³, E. Rizvi⁷⁵, S.H. Robertson^{86,j}, A. Robichaud-Veronneau¹¹⁹, D. Robinson²⁸, J.E.M. Robinson⁸³, A. Robson⁵³,

J.G. Rocha de Lima¹⁰⁷, C. Roda^{123a,123b}, D. Roda Dos Santos³⁰, A. Roe⁵⁴, S. Roe³⁰, O. Røhne¹¹⁸, S. Rolli¹⁶², A. Romaniouk⁹⁷, M. Romano^{20a,20b}, G. Romeo²⁷, E. Romero Adam¹⁶⁸, N. Rompotis¹³⁹, L. Roos⁷⁹, E. Ros¹⁶⁸, S. Rosati^{133a}, K. Rosbach⁴⁹, A. Rose¹⁵⁰, M. Rose⁷⁶, G.A. Rosenbaum¹⁵⁹, P.L. Rosendahl¹⁴, O. Rosenthal¹⁴², V. Rossetti¹², E. Rossi^{133a,133b}, L.P. Rossi^{50a}, M. Rotaru^{26a}, I. Roth¹⁷³, J. Rothberg¹³⁹, D. Rousseau¹¹⁶, C.R. Royon¹³⁷, A. Rozanov⁸⁴, Y. Rozen¹⁵³, X. Ruan^{146c}, F. Rubbo¹², I. Rubinskiy⁴², N. Ruckstuhl¹⁰⁶, V.I. Rud⁹⁸, C. Rudolph⁴⁴, M.S. Rudolph¹⁵⁹, F. Rühr⁷, A. Ruiz-Martinez⁶³, L. Romyantsev⁶⁴, Z. Rurikova⁴⁸, N.A. Rusakovich⁶⁴, A. Ruschke⁹⁹, J.P. Rutherford⁷, N. Ruthmann⁴⁸, P. Ruzicka¹²⁶, Y.F. Ryabov¹²², M. Rybar¹²⁸, G. Rybkin¹¹⁶, N.C. Ryder¹¹⁹, A.F. Saavedra¹⁵¹, A. Saddique³, I. Sadeh¹⁵⁴, H.F.W. Sadrozinski¹³⁸, R. Sadykov⁶⁴, F. Safai Tehrani^{133a}, H. Sakamoto¹⁵⁶, G. Salamanna⁷⁵, A. Salamon^{134a}, M. Saleem¹¹², D. Salek³⁰, D. Salihagic¹⁰⁰, A. Salnikov¹⁴⁴, J. Salt¹⁶⁸, B.M. Salvachua Ferrando⁶, D. Salvatore^{37a,37b}, F. Salvatore¹⁵⁰, A. Salvucci¹⁰⁵, A. Salzburger³⁰, D. Sampsonidis¹⁵⁵, A. Sanchez^{103a,103b}, J. Sánchez¹⁶⁸, V. Sanchez Martinez¹⁶⁸, H. Sandaker¹⁴, H.G. Sander⁸², M.P. Sanders⁹⁹, M. Sandhoff¹⁷⁶, T. Sandoval²⁸, C. Sandoval¹⁶³, R. Sandstroem¹⁰⁰, D.P.C. Sankey¹³⁰, A. Sansoni⁴⁷, C. Santoni³⁴, R. Santonico^{134a,134b}, H. Santos^{125a}, I. Santoyo Castillo¹⁵⁰, K. Sapp¹²⁴, J.G. Saraiva^{125a}, T. Sarangi¹⁷⁴, E. Sarkisyan-Grinbaum⁸, B. Sarrazin²¹, F. Sarri^{123a,123b}, G. Sartisohn¹⁷⁶, O. Sasaki⁶⁵, Y. Sasaki¹⁵⁶, N. Sasao⁶⁷, I. Satsounkevitch⁹¹, G. Sauvage^{5,*}, E. Sauvan⁵, J.B. Sauvan¹¹⁶, P. Savard^{159,e}, V. Savinov¹²⁴, D.O. Savu³⁰, C. Sawyer¹¹⁹, L. Sawyer^{78,l}, D.H. Saxon⁵³, J. Saxon¹²¹, C. Sbarra^{20a}, A. Sbrizzi³, D.A. Scannicchio¹⁶⁴, M. Scarcella¹⁵¹, J. Schaarschmidt¹¹⁶, P. Schacht¹⁰⁰, D. Schaefer¹²¹, A. Schaelicke⁴⁶, S. Schaepe²¹, S. Schaezel^{58b}, U. Schäfer⁸², A.C. Schaffer¹¹⁶, D. Schaile⁹⁹, R.D. Schamberger¹⁴⁹, V. Scharf^{58a}, V.A. Schegelsky¹²², D. Scheirich⁸⁸, M. Schernau¹⁶⁴, M.I. Scherzer³⁵, C. Schiavi^{50a,50b}, J. Schieck⁹⁹, C. Schillo⁴⁸, M. Schioppa^{37a,37b}, S. Schlenker³⁰, E. Schmidt⁴⁸, K. Schmieden²¹, C. Schmitt⁸², C. Schmitt⁹⁹, S. Schmitt^{58b}, B. Schneider¹⁷, Y.J. Schnellbach⁷³, U. Schnoor⁴⁴, L. Schoeffel¹³⁷, A. Schoening^{58b}, A.L.S. Schorlemmer⁵⁴, M. Schott⁸², D. Schouten^{160a}, J. Schovancova¹²⁶, M. Schram⁸⁶, C. Schroeder⁸², N. Schroer^{58c}, M.J. Schultens²¹, H.-C. Schultz-Coulon^{58a}, H. Schulz¹⁶, M. Schumacher⁴⁸, B.A. Schumm¹³⁸, Ph. Schune¹³⁷, A. Schwartzman¹⁴⁴, Ph. Schwegler¹⁰⁰, Ph. Schwemling¹³⁷, R. Schwiendhorst⁸⁹, J. Schwindling¹³⁷, T. Schwindt²¹, M. Schwoerer⁵, F.G. Sciacca¹⁷, E. Scifo¹¹⁶, G. Sciolla²³, W.G. Scott¹³⁰, F. Scutti²¹, J. Searcy⁸⁸, G. Sedov⁴², E. Sedykh¹²², S.C. Seidel¹⁰⁴, A. Seiden¹³⁸, F. Seifert⁴⁴, J.M. Seixas^{24a}, G. Sekhniaidze^{103a}, S.J. Sekula⁴⁰, K.E. Selbach⁴⁶, D.M. Seliverstov¹²², G. Sellers⁷³, M. Seman^{145b}, N. Semprini-Cesari^{20a,20b}, C. Serfon³⁰, L. Serin¹¹⁶, L. Serkin⁵⁴, T. Serre⁸⁴, R. Seuster^{160a}, H. Severini¹¹², A. Sfyrila³⁰, E. Shabalina⁵⁴, M. Shamim¹¹⁵, L.Y. Shan^{33a}, J.T. Shank²², Q.T. Shao⁸⁷, M. Shapiro¹⁵, P.B. Shatalov⁹⁶, K. Shaw^{165a,165c}, P. Sherwood⁷⁷, S. Shimizu¹⁰², M. Shimojima¹⁰¹, T. Shin⁵⁶, M. Shiyakova⁶⁴, A. Shmeleva⁹⁵, M.J. Shochet³¹, D. Short¹¹⁹, S. Shrestha⁶³, E. Shulga⁹⁷, M.A. Shupe⁷, P. Sicho¹²⁶, A. Sidoti^{133a}, F. Siegert⁴⁸, Dj. Sijacki^{13a}, O. Silbert¹⁷³, J. Silva^{125a}, Y. Silver¹⁵⁴, D. Silverstein¹⁴⁴, S.B. Silverstein^{147a}, V. Simak¹²⁷, O. Simard⁵, Lj. Simic^{13a}, S. Simion¹¹⁶, E. Simioni⁸², B. Simmons⁷⁷, R. Simoniello^{90a,90b}, M. Simonyan³⁶, P. Sinervo¹⁵⁹, N.B. Sinev¹¹⁵, V. Sipica¹⁴², G. Siragusa¹⁷⁵, A. Sircar⁷⁸, A.N. Sisakyan^{64,*}, S.Yu. Sivoklokov⁹⁸, J. Sjölin^{147a,147b}, T.B. Sjursen¹⁴, L.A. Skinnari¹⁵, H.P. Skottowe⁵⁷, K. Skovpen¹⁰⁸, P. Skubic¹¹², M. Slater¹⁸, T. Slavicek¹²⁷, K. Sliwa¹⁶², V. Smakhtin¹⁷³, B.H. Smart⁴⁶, L. Smestad¹¹⁸, S.Yu. Smirnov⁹⁷, Y. Smirnov⁹⁷, L.N. Smirnova^{98,ai}, O. Smirnova⁸⁰, K.M. Smith⁵³, M. Smizanska⁷¹, K. Smolek¹²⁷, A.A. Snesarev⁹⁵, G. Snidero⁷⁵, J. Snow¹¹², S. Snyder²⁵, R. Sobie^{170,j}, J. Sodomka¹²⁷, A. Soffer¹⁵⁴, D.A. Soh^{152,u}, C.A. Solans³⁰, M. Solar¹²⁷, J. Solc¹²⁷, E.Yu. Soldatov⁹⁷, U. Soldevila¹⁶⁸, E. Solfaroli Camillocci^{133a,133b}, A.A. Solodkov¹²⁹, O.V. Solovyanov¹²⁹, V. Solovyev¹²², N. Soni¹, A. Sood¹⁵, V. Sopko¹²⁷, B. Sopko¹²⁷, M. Sosebee⁸, R. Soualah^{165a,165c}, P. Soueid⁹⁴, A. Soukharev¹⁰⁸, D. South⁴², S. Spagnolo^{72a,72b}, F. Spano⁷⁶, R. Spighi^{20a}, G. Spigo³⁰, R. Spiwoks³⁰, M. Spousta^{128,aj}, T. Spreitzer¹⁵⁹, B. Spurlock⁸, R.D. St. Denis⁵³, J. Stahlman¹²¹, R. Stamen^{58a}, E. Stanecka³⁹, R.W. Stanek⁶, C. Stanescu^{135a}, M. Stanescu-Bellu⁴², M.M. Stanitzki⁴², S. Stapnes¹¹⁸, E.A. Starchenko¹²⁹, J. Stark⁵⁵, P. Staroba¹²⁶, P. Starovoitov⁴², R. Staszewski³⁹, A. Staude⁹⁹, P. Stavina^{145a,*}, G. Steele⁵³, P. Steinbach⁴⁴, P. Steinberg²⁵, I. Stekl¹²⁷, B. Stelzer¹⁴³, H.J. Stelzer⁸⁹,

O. Stelzer-Chilton^{160a}, H. Stenzel⁵², S. Stern¹⁰⁰, G.A. Stewart³⁰, J.A. Stillings²¹, M.C. Stockton⁸⁶, M. Stoebe⁸⁶, K. Stoerig⁴⁸, G. Stoicea^{26a}, S. Stonjek¹⁰⁰, A.R. Stradling⁸, A. Straessner⁴⁴, J. Strandberg¹⁴⁸, S. Strandberg^{147a,147b}, A. Strandlie¹¹⁸, M. Strang¹¹⁰, E. Strauss¹⁴⁴, M. Strauss¹¹², P. Strizenc^{145b}, R. Ströhmer¹⁷⁵, D.M. Strom¹¹⁵, J.A. Strong^{76,*}, R. Stroynowski⁴⁰, B. Stugu¹⁴, I. Stumer^{25,*}, J. Stupak¹⁴⁹, P. Sturm¹⁷⁶, N.A. Styles⁴², D. Su¹⁴⁴, H.S. Subramania³, R. Subramaniam⁷⁸, A. Succurro¹², Y. Sugaya¹¹⁷, C. Suhr¹⁰⁷, M. Suk¹²⁷, V.V. Sulin⁹⁵, S. Sultansoy^{4c}, T. Sumida⁶⁷, X. Sun⁵⁵, J.E. Sundermann⁴⁸, K. Suruliz¹⁴⁰, G. Susinno^{37a,37b}, M.R. Sutton¹⁵⁰, Y. Suzuki⁶⁵, Y. Suzuki⁶⁶, M. Svatos¹²⁶, S. Swedish¹⁶⁹, M. Swiatlowski¹⁴⁴, I. Sykora^{145a}, T. Sykora¹²⁸, D. Ta¹⁰⁶, K. Tackmann⁴², A. Taffard¹⁶⁴, R. Tafirout^{160a}, N. Taiblum¹⁵⁴, Y. Takahashi¹⁰², H. Takai²⁵, R. Takashima⁶⁸, H. Takeda⁶⁶, T. Takeshita¹⁴¹, Y. Takubo⁶⁵, M. Talby⁸⁴, A. Talyshev^{108,g}, J.Y.C. Tam¹⁷⁵, M.C. Tamsett^{78,ak}, K.G. Tan⁸⁷, J. Tanaka¹⁵⁶, R. Tanaka¹¹⁶, S. Tanaka¹³², S. Tanaka⁶⁵, A.J. Tanasijczuk¹⁴³, K. Tani⁶⁶, N. Tannoury⁸⁴, S. Tapprogge⁸², S. Tarem¹⁵³, F. Tarrade²⁹, G.F. Tartarelli^{90a}, P. Tas¹²⁸, M. Tasevsky¹²⁶, T. Tashiro⁶⁷, E. Tassi^{37a,37b}, Y. Tayalati^{136d}, C. Taylor⁷⁷, F.E. Taylor⁹³, G.N. Taylor⁸⁷, W. Taylor^{160b}, M. Teinturier¹¹⁶, F.A. Teischinger³⁰, M. Teixeira Dias Castanheira⁷⁵, P. Teixeira-Dias⁷⁶, K.K. Temming⁴⁸, H. Ten Kate³⁰, P.K. Teng¹⁵², S. Terada⁶⁵, K. Terashi¹⁵⁶, J. Terron⁸¹, M. Testa⁴⁷, R.J. Teuscher^{159,j}, J. Therhaag²¹, T. Theveneaux-Pelzer³⁴, S. Thoma⁴⁸, J.P. Thomas¹⁸, E.N. Thompson³⁵, P.D. Thompson¹⁸, P.D. Thompson¹⁵⁹, A.S. Thompson⁵³, L.A. Thomsen³⁶, E. Thomson¹²¹, M. Thomson²⁸, W.M. Thong⁸⁷, R.P. Thun^{88,*}, F. Tian³⁵, M.J. Tibbetts¹⁵, T. Tic¹²⁶, V.O. Tikhomirov⁹⁵, Y.A. Tikhonov^{108,g}, S. Timoshenko⁹⁷, E. Tiouchichine⁸⁴, P. Tipton¹⁷⁷, S. Tisserant⁸⁴, T. Todorov⁵, S. Todorova-Nova¹⁶², B. Toggerson¹⁶⁴, J. Tojo⁶⁹, S. Tokár^{145a}, K. Tokushuku⁶⁵, K. Tollefson⁸⁹, L. Tomlinson⁸³, M. Tomoto¹⁰², L. Tompkins³¹, K. Toms¹⁰⁴, A. Tonoyan¹⁴, C. Topfel¹⁷, N.D. Topilin⁶⁴, E. Torrence¹¹⁵, H. Torres⁷⁹, E. Torró Pastor¹⁶⁸, J. Toth^{84,af}, F. Touchard⁸⁴, D.R. Tovey¹⁴⁰, H.L. Tran¹¹⁶, T. Trefzger¹⁷⁵, L. Tremblet³⁰, A. Tricoli³⁰, I.M. Trigger^{160a}, S. Trincaz-Duvoid⁷⁹, M.F. Tripiana⁷⁰, N. Triplett²⁵, W. Trischuk¹⁵⁹, B. Trocmé⁵⁵, C. Troncon^{90a}, M. Trotter-McDonald¹⁴³, M. Trovatelli^{135a,135b}, P. True⁸⁹, M. Trzebinski³⁹, A. Trzupek³⁹, C. Tsarouchas³⁰, J.C-L. Tseng¹¹⁹, M. Tsiakiris¹⁰⁶, P.V. Tsiarehka⁹¹, D. Tsionou¹³⁷, G. Tsipolitis¹⁰, S. Tsiskaridze¹², V. Tsiskaridze⁴⁸, E.G. Tskhadadze^{51a}, I.I. Tsukerman⁹⁶, V. Tsulaia¹⁵, J.-W. Tsung²¹, S. Tsuno⁶⁵, D. Tsybychev¹⁴⁹, A. Tua¹⁴⁰, A. Tudorache^{26a}, V. Tudorache^{26a}, J.M. Tuggle³¹, A.N. Tuna¹²¹, M. Turala³⁹, D. Turecek¹²⁷, I. Turk Cakir^{4d}, R. Turra^{90a,90b}, P.M. Tuts³⁵, A. Tykhonov⁷⁴, M. Tylmad^{147a,147b}, M. Tyndel¹³⁰, K. Uchida²¹, I. Ueda¹⁵⁶, R. Ueno²⁹, M. Ughetto⁸⁴, M. Ugland¹⁴, M. Uhlenbrock²¹, F. Ukegawa¹⁶¹, G. Unal³⁰, A. Undrus²⁵, G. Unel¹⁶⁴, F.C. Ungaro⁴⁸, Y. Unno⁶⁵, D. Urbaniec³⁵, P. Urquijo²¹, G. Usai⁸, L. Vacavant⁸⁴, V. Vacek¹²⁷, B. Vachon⁸⁶, S. Vahsen¹⁵, N. Valencic¹⁰⁶, S. Valentineti^{20a,20b}, A. Valero¹⁶⁸, L. Valery³⁴, S. Valkar¹²⁸, E. Valladolid Gallego¹⁶⁸, S. Vallecorsa¹⁵³, J.A. Valls Ferrer¹⁶⁸, R. Van Berg¹²¹, P.C. Van Der Deijl¹⁰⁶, R. van der Geer¹⁰⁶, H. van der Graaf¹⁰⁶, R. Van Der Leeuw¹⁰⁶, D. van der Ster³⁰, N. van Eldik³⁰, P. van Gemmeren⁶, J. Van Nieuwkoop¹⁴³, I. van Vulpen¹⁰⁶, M. Vanadia¹⁰⁰, W. Vandelli³⁰, A. Vaniachine⁶, P. Vankov⁴², F. Vannucci⁷⁹, R. Vari^{133a}, E.W. Varnes⁷, T. Varol⁸⁵, D. Varouchas¹⁵, A. Vartapetian⁸, K.E. Varvell¹⁵¹, V.I. Vassilakopoulos⁵⁶, F. Vazeille³⁴, T. Vazquez Schroeder⁵⁴, F. Veloso^{125a}, S. Veneziano^{133a}, A. Ventura^{72a,72b}, D. Ventura⁸⁵, M. Venturi⁴⁸, N. Venturi¹⁵⁹, V. Vercesi^{120a}, M. Verducci¹³⁹, W. Verkerke¹⁰⁶, J.C. Vermeulen¹⁰⁶, A. Vest⁴⁴, M.C. Vetterli^{143,e}, I. Vichou¹⁶⁶, T. Vickey^{146c,al}, O.E. Vickey Boeriu^{146c}, G.H.A. Viehhauser¹¹⁹, S. Viel¹⁶⁹, M. Villa^{20a,20b}, M. Villaplana Perez¹⁶⁸, E. Vilucchi⁴⁷, M.G. Vincter²⁹, V.B. Vinogradov⁶⁴, J. Virzi¹⁵, O. Vitells¹⁷³, M. Viti⁴², I. Vivarelli⁴⁸, F. Vives Vaque³, S. Vlachos¹⁰, D. Vladioiu⁹⁹, M. Vlasak¹²⁷, A. Vogel²¹, P. Vokac¹²⁷, G. Volpi⁴⁷, M. Volpi⁸⁷, G. Volpini^{90a}, H. von der Schmitt¹⁰⁰, H. von Radziewski⁴⁸, E. von Toerne²¹, V. Vorobel¹²⁸, M. Vos¹⁶⁸, R. Voss³⁰, J.H. Vossebeld⁷³, N. Vranjes¹³⁷, M. Vranjes Milosavljevic¹⁰⁶, V. Vrba¹²⁶, M. Vreeswijk¹⁰⁶, T. Vu Anh⁴⁸, R. Vuillermet³⁰, I. Vukotic³¹, Z. Vykydal¹²⁷, W. Wagner¹⁷⁶, P. Wagner²¹, S. Wahrmund⁴⁴, J. Wakabayashi¹⁰², S. Walch⁸⁸, J. Walder⁷¹, R. Walker⁹⁹, W. Walkowiak¹⁴², R. Wall¹⁷⁷, P. Waller⁷³, B. Walsh¹⁷⁷, C. Wang⁴⁵, H. Wang¹⁷⁴, H. Wang⁴⁰, J. Wang¹⁵², J. Wang^{33a}, K. Wang⁸⁶, R. Wang¹⁰⁴, S.M. Wang¹⁵², T. Wang²¹, X. Wang¹⁷⁷, A. Warburton⁸⁶, C.P. Ward²⁸, D.R. Wardrope⁷⁷,

M. Warsinsky⁴⁸, A. Washbrook⁴⁶, C. Wasicki⁴², I. Watanabe⁶⁶, P.M. Watkins¹⁸, A.T. Watson¹⁸, I.J. Watson¹⁵¹, M.F. Watson¹⁸, G. Watts¹³⁹, S. Watts⁸³, A.T. Waugh¹⁵¹, B.M. Waugh⁷⁷, M.S. Weber¹⁷, J.S. Webster³¹, A.R. Weidberg¹¹⁹, P. Weigell¹⁰⁰, J. Weingarten⁵⁴, C. Weiser⁴⁸, P.S. Wells³⁰, T. Wenaus²⁵, D. Wendland¹⁶, Z. Weng^{152,u}, T. Wengler³⁰, S. Wenig³⁰, N. Vermes²¹, M. Werner⁴⁸, P. Werner³⁰, M. Werth¹⁶⁴, M. Wessels^{58a}, J. Wetter¹⁶², K. Whalen²⁹, A. White⁸, M.J. White⁸⁷, R. White^{32b}, S. White^{123a,123b}, S.R. Whitehead¹¹⁹, D. Whiteson¹⁶⁴, D. Whittington⁶⁰, D. Wicke¹⁷⁶, F.J. Wickens¹³⁰, W. Wiedenmann¹⁷⁴, M. Wielers^{80,d}, P. Wienemann²¹, C. Wigglesworth³⁶, L.A.M. Wiik-Fuchs²¹, P.A. Wijeratne⁷⁷, A. Wildauer¹⁰⁰, M.A. Wildt^{42,r}, I. Wilhelm¹²⁸, H.G. Wilkens³⁰, J.Z. Will⁹⁹, E. Williams³⁵, H.H. Williams¹²¹, S. Williams²⁸, W. Willis^{35,*}, S. Willocq⁸⁵, J.A. Wilson¹⁸, A. Wilson⁸⁸, I. Wingerter-Seez⁵, S. Winkelmann⁴⁸, F. Winklmeier³⁰, M. Wittgen¹⁴⁴, T. Wittig⁴³, J. Wittkowski⁹⁹, S.J. Wollstadt⁸², M.W. Wolter³⁹, H. Wolters^{125a,h}, W.C. Wong⁴¹, G. Wooden⁸⁸, B.K. Wosiek³⁹, J. Wotschack³⁰, M.J. Woudstra⁸³, K.W. Wozniak³⁹, K. Wraight⁵³, M. Wright⁵³, B. Wrona⁷³, S.L. Wu¹⁷⁴, X. Wu⁴⁹, Y. Wu⁸⁸, E. Wulf³⁵, B.M. Wynne⁴⁶, S. Xella³⁶, M. Xiao¹³⁷, S. Xie⁴⁸, C. Xu^{33b,z}, D. Xu^{33a}, L. Xu^{33b}, B. Yabsley¹⁵¹, S. Yacoob^{146b,am}, M. Yamada⁶⁵, H. Yamaguchi¹⁵⁶, Y. Yamaguchi¹⁵⁶, A. Yamamoto⁶⁵, K. Yamamoto⁶³, S. Yamamoto¹⁵⁶, T. Yamamura¹⁵⁶, T. Yamanaka¹⁵⁶, K. Yamauchi¹⁰², T. Yamazaki¹⁵⁶, Y. Yamazaki⁶⁶, Z. Yan²², H. Yang^{33e}, H. Yang¹⁷⁴, U.K. Yang⁸³, Y. Yang¹¹⁰, Z. Yang^{147a,147b}, S. Yanush⁹², L. Yao^{33a}, Y. Yasu⁶⁵, E. Yatsenko⁴², K.H. Yau Wong²¹, J. Ye⁴⁰, S. Ye²⁵, A.L. Yen⁵⁷, E. Yildirim⁴², M. Yilmaz^{4b}, R. Yoosofmiya¹²⁴, K. Yorita¹⁷², R. Yoshida⁶, K. Yoshihara¹⁵⁶, C. Young¹⁴⁴, C.J.S. Young¹¹⁹, S. Youssef²², D. Yu²⁵, D.R. Yu¹⁵, J. Yu⁸, J. Yu¹¹³, L. Yuan⁶⁶, A. Yurkewicz¹⁰⁷, B. Zabinski³⁹, R. Zaidan⁶², A.M. Zaitsev^{129,aa}, S. Zambito²³, L. Zanello^{133a,133b}, D. Zanzi¹⁰⁰, A. Zaytsev²⁵, C. Zeitnitz¹⁷⁶, M. Zeman¹²⁷, A. Zemla³⁹, O. Zenin¹²⁹, T. Ženiš^{145a}, D. Zerwas¹¹⁶, G. Zevi della Porta⁵⁷, D. Zhang⁸⁸, H. Zhang⁸⁹, J. Zhang⁶, L. Zhang¹⁵², X. Zhang^{33d}, Z. Zhang¹¹⁶, Z. Zhao^{33b}, A. Zhemchugov⁶⁴, J. Zhong¹¹⁹, B. Zhou⁸⁸, N. Zhou¹⁶⁴, Y. Zhou¹⁵², C.G. Zhu^{33d}, H. Zhu⁴², J. Zhu⁸⁸, Y. Zhu^{33b}, X. Zhuang^{33a}, A. Zibell⁹⁹, D. Ziemska⁶⁰, N.I. Zimin⁶⁴, C. Zimmermann⁸², R. Zimmermann²¹, S. Zimmermann²¹, S. Zimmermann⁴⁸, Z. Zinonos^{123a,123b}, M. Ziolkowski¹⁴², R. Zitoun⁵, L. Živković³⁵, V.V. Zmouchko^{129,*}, G. Zobernig¹⁷⁴, A. Zoccoli^{20a,20b}, M. zur Nedden¹⁶, V. Zutshi¹⁰⁷, L. Zwalinski³⁰.

¹ School of Chemistry and Physics, University of Adelaide, Adelaide, Australia

² Physics Department, SUNY Albany, Albany NY, United States of America

³ Department of Physics, University of Alberta, Edmonton AB, Canada

⁴ (a) Department of Physics, Ankara University, Ankara; (b) Department of Physics, Gazi University, Ankara; (c) Division of Physics, TOBB University of Economics and Technology, Ankara; (d) Turkish Atomic Energy Authority, Ankara, Turkey

⁵ LAPP, CNRS/IN2P3 and Université de Savoie, Annecy-le-Vieux, France

⁶ High Energy Physics Division, Argonne National Laboratory, Argonne IL, United States of America

⁷ Department of Physics, University of Arizona, Tucson AZ, United States of America

⁸ Department of Physics, The University of Texas at Arlington, Arlington TX, United States of America

⁹ Physics Department, University of Athens, Athens, Greece

¹⁰ Physics Department, National Technical University of Athens, Zografou, Greece

¹¹ Institute of Physics, Azerbaijan Academy of Sciences, Baku, Azerbaijan

¹² Institut de Física d'Altes Energies and Departament de Física de la Universitat Autònoma de Barcelona and ICREA, Barcelona, Spain

¹³ (a) Institute of Physics, University of Belgrade, Belgrade; (b) Vinca Institute of Nuclear Sciences, University of Belgrade, Belgrade, Serbia

¹⁴ Department for Physics and Technology, University of Bergen, Bergen, Norway

¹⁵ Physics Division, Lawrence Berkeley National Laboratory and University of California, Berkeley CA, United States of America

¹⁶ Department of Physics, Humboldt University, Berlin, Germany

- 17 *Albert Einstein Center for Fundamental Physics and Laboratory for High Energy Physics, University of Bern, Bern, Switzerland*
- 18 *School of Physics and Astronomy, University of Birmingham, Birmingham, United Kingdom*
- 19 ^(a)*Department of Physics, Bogazici University, Istanbul;* ^(b)*Department of Physics, Dogus University, Istanbul;* ^(c)*Department of Physics Engineering, Gaziantep University, Gaziantep, Turkey*
- 20 ^(a)*INFN Sezione di Bologna;* ^(b)*Dipartimento di Fisica, Università di Bologna, Bologna, Italy*
- 21 *Physikalisches Institut, University of Bonn, Bonn, Germany*
- 22 *Department of Physics, Boston University, Boston MA, United States of America*
- 23 *Department of Physics, Brandeis University, Waltham MA, United States of America*
- 24 ^(a)*Universidade Federal do Rio De Janeiro COPPE/EE/IF, Rio de Janeiro;* ^(b)*Federal University of Juiz de Fora (UFJF), Juiz de Fora;* ^(c)*Federal University of Sao Joao del Rei (UFSJ), Sao Joao del Rei;* ^(d)*Instituto de Física, Universidade de Sao Paulo, Sao Paulo, Brazil*
- 25 *Physics Department, Brookhaven National Laboratory, Upton NY, United States of America*
- 26 ^(a)*National Institute of Physics and Nuclear Engineering, Bucharest;* ^(b)*National Institute for Research and Development of Isotopic and Molecular Technologies, Physics Department, Cluj Napoca;* ^(c)*University Politehnica Bucharest, Bucharest;* ^(d)*West University in Timisoara, Timisoara, Romania*
- 27 *Departamento de Física, Universidad de Buenos Aires, Buenos Aires, Argentina*
- 28 *Cavendish Laboratory, University of Cambridge, Cambridge, United Kingdom*
- 29 *Department of Physics, Carleton University, Ottawa ON, Canada*
- 30 *CERN, Geneva, Switzerland*
- 31 *Enrico Fermi Institute, University of Chicago, Chicago IL, United States of America*
- 32 ^(a)*Departamento de Física, Pontificia Universidad Católica de Chile, Santiago;* ^(b)*Departamento de Física, Universidad Técnica Federico Santa María, Valparaiso, Chile*
- 33 ^(a)*Institute of High Energy Physics, Chinese Academy of Sciences, Beijing;* ^(b)*Department of Modern Physics, University of Science and Technology of China, Anhui;* ^(c)*Department of Physics, Nanjing University, Jiangsu;* ^(d)*School of Physics, Shandong University, Shandong;* ^(e)*Physics Department, Shanghai Jiao Tong University, Shanghai, China*
- 34 *Laboratoire de Physique Corpusculaire, Clermont Université and Université Blaise Pascal and CNRS/IN2P3, Clermont-Ferrand, France*
- 35 *Nevis Laboratory, Columbia University, Irvington NY, United States of America*
- 36 *Niels Bohr Institute, University of Copenhagen, Kobenhavn, Denmark*
- 37 ^(a)*INFN Gruppo Collegato di Cosenza;* ^(b)*Dipartimento di Fisica, Università della Calabria, Rende, Italy*
- 38 ^(a)*AGH University of Science and Technology, Faculty of Physics and Applied Computer Science, Krakow;* ^(b)*Marian Smoluchowski Institute of Physics, Jagiellonian University, Krakow, Poland*
- 39 *The Henryk Niewodniczanski Institute of Nuclear Physics, Polish Academy of Sciences, Krakow, Poland*
- 40 *Physics Department, Southern Methodist University, Dallas TX, United States of America*
- 41 *Physics Department, University of Texas at Dallas, Richardson TX, United States of America*
- 42 *DESY, Hamburg and Zeuthen, Germany*
- 43 *Institut für Experimentelle Physik IV, Technische Universität Dortmund, Dortmund, Germany*
- 44 *Institut für Kern- und Teilchenphysik, Technical University Dresden, Dresden, Germany*
- 45 *Department of Physics, Duke University, Durham NC, United States of America*
- 46 *SUPA - School of Physics and Astronomy, University of Edinburgh, Edinburgh, United Kingdom*
- 47 *INFN Laboratori Nazionali di Frascati, Frascati, Italy*
- 48 *Fakultät für Mathematik und Physik, Albert-Ludwigs-Universität, Freiburg, Germany*
- 49 *Section de Physique, Université de Genève, Geneva, Switzerland*
- 50 ^(a)*INFN Sezione di Genova;* ^(b)*Dipartimento di Fisica, Università di Genova, Genova, Italy*
- 51 ^(a)*E. Andronikashvili Institute of Physics, Iv. Javakhishvili Tbilisi State University, Tbilisi;* ^(b)*High Energy Physics Institute, Tbilisi State University, Tbilisi, Georgia*
- 52 *II Physikalisches Institut, Justus-Liebig-Universität Giessen, Giessen, Germany*
- 53 *SUPA - School of Physics and Astronomy, University of Glasgow, Glasgow, United Kingdom*
- 54 *II Physikalisches Institut, Georg-August-Universität, Göttingen, Germany*
- 55 *Laboratoire de Physique Subatomique et de Cosmologie, Université Joseph Fourier and CNRS/IN2P3 and Institut National Polytechnique de Grenoble, Grenoble, France*

- 56 *Department of Physics, Hampton University, Hampton VA, United States of America*
- 57 *Laboratory for Particle Physics and Cosmology, Harvard University, Cambridge MA, United States of America*
- 58 ^(a)*Kirchhoff-Institut für Physik, Ruprecht-Karls-Universität Heidelberg, Heidelberg;* ^(b)*Physikalisches Institut, Ruprecht-Karls-Universität Heidelberg, Heidelberg;* ^(c)*ZITI Institut für technische Informatik, Ruprecht-Karls-Universität Heidelberg, Mannheim, Germany*
- 59 *Faculty of Applied Information Science, Hiroshima Institute of Technology, Hiroshima, Japan*
- 60 *Department of Physics, Indiana University, Bloomington IN, United States of America*
- 61 *Institut für Astro- und Teilchenphysik, Leopold-Franzens-Universität, Innsbruck, Austria*
- 62 *University of Iowa, Iowa City IA, United States of America*
- 63 *Department of Physics and Astronomy, Iowa State University, Ames IA, United States of America*
- 64 *Joint Institute for Nuclear Research, JINR Dubna, Dubna, Russia*
- 65 *KEK, High Energy Accelerator Research Organization, Tsukuba, Japan*
- 66 *Graduate School of Science, Kobe University, Kobe, Japan*
- 67 *Faculty of Science, Kyoto University, Kyoto, Japan*
- 68 *Kyoto University of Education, Kyoto, Japan*
- 69 *Department of Physics, Kyushu University, Fukuoka, Japan*
- 70 *Instituto de Física La Plata, Universidad Nacional de La Plata and CONICET, La Plata, Argentina*
- 71 *Physics Department, Lancaster University, Lancaster, United Kingdom*
- 72 ^(a)*INFN Sezione di Lecce;* ^(b)*Dipartimento di Matematica e Fisica, Università del Salento, Lecce, Italy*
- 73 *Oliver Lodge Laboratory, University of Liverpool, Liverpool, United Kingdom*
- 74 *Department of Physics, Jožef Stefan Institute and University of Ljubljana, Ljubljana, Slovenia*
- 75 *School of Physics and Astronomy, Queen Mary University of London, London, United Kingdom*
- 76 *Department of Physics, Royal Holloway University of London, Surrey, United Kingdom*
- 77 *Department of Physics and Astronomy, University College London, London, United Kingdom*
- 78 *Louisiana Tech University, Ruston LA, United States of America*
- 79 *Laboratoire de Physique Nucléaire et de Hautes Energies, UPMC and Université Paris-Diderot and CNRS/IN2P3, Paris, France*
- 80 *Fysiska institutionen, Lunds universitet, Lund, Sweden*
- 81 *Departamento de Física Teórica C-15, Universidad Autónoma de Madrid, Madrid, Spain*
- 82 *Institut für Physik, Universität Mainz, Mainz, Germany*
- 83 *School of Physics and Astronomy, University of Manchester, Manchester, United Kingdom*
- 84 *CPPM, Aix-Marseille Université et CNRS/IN2P3, Marseille, France*
- 85 *Department of Physics, University of Massachusetts, Amherst MA, United States of America*
- 86 *Department of Physics, McGill University, Montreal QC, Canada*
- 87 *School of Physics, University of Melbourne, Victoria, Australia*
- 88 *Department of Physics, The University of Michigan, Ann Arbor MI, United States of America*
- 89 *Department of Physics and Astronomy, Michigan State University, East Lansing MI, United States of America*
- 90 ^(a)*INFN Sezione di Milano;* ^(b)*Dipartimento di Fisica, Università di Milano, Milano, Italy*
- 91 *B.I. Stepanov Institute of Physics, National Academy of Sciences of Belarus, Minsk, Republic of Belarus*
- 92 *National Scientific and Educational Centre for Particle and High Energy Physics, Minsk, Republic of Belarus*
- 93 *Department of Physics, Massachusetts Institute of Technology, Cambridge MA, United States of America*
- 94 *Group of Particle Physics, University of Montreal, Montreal QC, Canada*
- 95 *P.N. Lebedev Institute of Physics, Academy of Sciences, Moscow, Russia*
- 96 *Institute for Theoretical and Experimental Physics (ITEP), Moscow, Russia*
- 97 *Moscow Engineering and Physics Institute (MEPhI), Moscow, Russia*
- 98 *D.V.Skobeltzyn Institute of Nuclear Physics, M.V.Lomonosov Moscow State University, Moscow, Russia*
- 99 *Fakultät für Physik, Ludwig-Maximilians-Universität München, München, Germany*
- 100 *Max-Planck-Institut für Physik (Werner-Heisenberg-Institut), München, Germany*
- 101 *Nagasaki Institute of Applied Science, Nagasaki, Japan*
- 102 *Graduate School of Science and Kobayashi-Maskawa Institute, Nagoya University, Nagoya, Japan*
- 103 ^(a)*INFN Sezione di Napoli;* ^(b)*Dipartimento di Scienze Fisiche, Università di Napoli, Napoli, Italy*
- 104 *Department of Physics and Astronomy, University of New Mexico, Albuquerque NM, United States of America*

- 105 *Institute for Mathematics, Astrophysics and Particle Physics, Radboud University Nijmegen/Nikhef, Nijmegen, Netherlands*
- 106 *Nikhef National Institute for Subatomic Physics and University of Amsterdam, Amsterdam, Netherlands*
- 107 *Department of Physics, Northern Illinois University, DeKalb IL, United States of America*
- 108 *Budker Institute of Nuclear Physics, SB RAS, Novosibirsk, Russia*
- 109 *Department of Physics, New York University, New York NY, United States of America*
- 110 *Ohio State University, Columbus OH, United States of America*
- 111 *Faculty of Science, Okayama University, Okayama, Japan*
- 112 *Homer L. Dodge Department of Physics and Astronomy, University of Oklahoma, Norman OK, United States of America*
- 113 *Department of Physics, Oklahoma State University, Stillwater OK, United States of America*
- 114 *Palacký University, RCPTM, Olomouc, Czech Republic*
- 115 *Center for High Energy Physics, University of Oregon, Eugene OR, United States of America*
- 116 *LAL, Université Paris-Sud and CNRS/IN2P3, Orsay, France*
- 117 *Graduate School of Science, Osaka University, Osaka, Japan*
- 118 *Department of Physics, University of Oslo, Oslo, Norway*
- 119 *Department of Physics, Oxford University, Oxford, United Kingdom*
- 120 ^(a)*INFN Sezione di Pavia;* ^(b)*Dipartimento di Fisica, Università di Pavia, Pavia, Italy*
- 121 *Department of Physics, University of Pennsylvania, Philadelphia PA, United States of America*
- 122 *Petersburg Nuclear Physics Institute, Gatchina, Russia*
- 123 ^(a)*INFN Sezione di Pisa;* ^(b)*Dipartimento di Fisica E. Fermi, Università di Pisa, Pisa, Italy*
- 124 *Department of Physics and Astronomy, University of Pittsburgh, Pittsburgh PA, United States of America*
- 125 ^(a)*Laboratorio de Instrumentacao e Fisica Experimental de Particulas - LIP, Lisboa, Portugal;*
^(b)*Departamento de Fisica Teorica y del Cosmos and CAFPE, Universidad de Granada, Granada, Spain*
- 126 *Institute of Physics, Academy of Sciences of the Czech Republic, Praha, Czech Republic*
- 127 *Czech Technical University in Prague, Praha, Czech Republic*
- 128 *Faculty of Mathematics and Physics, Charles University in Prague, Praha, Czech Republic*
- 129 *State Research Center Institute for High Energy Physics, Protvino, Russia*
- 130 *Particle Physics Department, Rutherford Appleton Laboratory, Didcot, United Kingdom*
- 131 *Physics Department, University of Regina, Regina SK, Canada*
- 132 *Ritsumeikan University, Kusatsu, Shiga, Japan*
- 133 ^(a)*INFN Sezione di Roma I;* ^(b)*Dipartimento di Fisica, Università La Sapienza, Roma, Italy*
- 134 ^(a)*INFN Sezione di Roma Tor Vergata;* ^(b)*Dipartimento di Fisica, Università di Roma Tor Vergata, Roma, Italy*
- 135 ^(a)*INFN Sezione di Roma Tre;* ^(b)*Dipartimento di Matematica e Fisica, Università Roma Tre, Roma, Italy*
- 136 ^(a)*Faculté des Sciences Ain Chock, Réseau Universitaire de Physique des Hautes Energies - Université Hassan II, Casablanca;* ^(b)*Centre National de l'Energie des Sciences Techniques Nucleaires, Rabat;* ^(c)*Faculté des Sciences Semlalia, Université Cadi Ayyad, LPHEA-Marrakech;* ^(d)*Faculté des Sciences, Université Mohamed Premier and LTPM, Oujda;* ^(e)*Faculté des sciences, Université Mohammed V-Agdal, Rabat, Morocco*
- 137 *DSM/IRFU (Institut de Recherches sur les Lois Fondamentales de l'Univers), CEA Saclay (Commissariat à l'Energie Atomique et aux Energies Alternatives), Gif-sur-Yvette, France*
- 138 *Santa Cruz Institute for Particle Physics, University of California Santa Cruz, Santa Cruz CA, United States of America*
- 139 *Department of Physics, University of Washington, Seattle WA, United States of America*
- 140 *Department of Physics and Astronomy, University of Sheffield, Sheffield, United Kingdom*
- 141 *Department of Physics, Shinshu University, Nagano, Japan*
- 142 *Fachbereich Physik, Universität Siegen, Siegen, Germany*
- 143 *Department of Physics, Simon Fraser University, Burnaby BC, Canada*
- 144 *SLAC National Accelerator Laboratory, Stanford CA, United States of America*
- 145 ^(a)*Faculty of Mathematics, Physics & Informatics, Comenius University, Bratislava;* ^(b)*Department of Subnuclear Physics, Institute of Experimental Physics of the Slovak Academy of Sciences, Kosice, Slovak Republic*

- 146 ^(a)Department of Physics, University of Cape Town, Cape Town; ^(b)Department of Physics, University of Johannesburg, Johannesburg; ^(c)School of Physics, University of the Witwatersrand, Johannesburg, South Africa
- 147 ^(a)Department of Physics, Stockholm University; ^(b)The Oskar Klein Centre, Stockholm, Sweden
- 148 Physics Department, Royal Institute of Technology, Stockholm, Sweden
- 149 Departments of Physics & Astronomy and Chemistry, Stony Brook University, Stony Brook NY, United States of America
- 150 Department of Physics and Astronomy, University of Sussex, Brighton, United Kingdom
- 151 School of Physics, University of Sydney, Sydney, Australia
- 152 Institute of Physics, Academia Sinica, Taipei, Taiwan
- 153 Department of Physics, Technion: Israel Institute of Technology, Haifa, Israel
- 154 Raymond and Beverly Sackler School of Physics and Astronomy, Tel Aviv University, Tel Aviv, Israel
- 155 Department of Physics, Aristotle University of Thessaloniki, Thessaloniki, Greece
- 156 International Center for Elementary Particle Physics and Department of Physics, The University of Tokyo, Tokyo, Japan
- 157 Graduate School of Science and Technology, Tokyo Metropolitan University, Tokyo, Japan
- 158 Department of Physics, Tokyo Institute of Technology, Tokyo, Japan
- 159 Department of Physics, University of Toronto, Toronto ON, Canada
- 160 ^(a)TRIUMF, Vancouver BC; ^(b)Department of Physics and Astronomy, York University, Toronto ON, Canada
- 161 Faculty of Pure and Applied Sciences, University of Tsukuba, Tsukuba, Japan
- 162 Department of Physics and Astronomy, Tufts University, Medford MA, United States of America
- 163 Centro de Investigaciones, Universidad Antonio Narino, Bogota, Colombia
- 164 Department of Physics and Astronomy, University of California Irvine, Irvine CA, United States of America
- 165 ^(a)INFN Gruppo Collegato di Udine; ^(b)ICTP, Trieste; ^(c)Dipartimento di Chimica, Fisica e Ambiente, Università di Udine, Udine, Italy
- 166 Department of Physics, University of Illinois, Urbana IL, United States of America
- 167 Department of Physics and Astronomy, University of Uppsala, Uppsala, Sweden
- 168 Instituto de Física Corpuscular (IFIC) and Departamento de Física Atómica, Molecular y Nuclear and Departamento de Ingeniería Electrónica and Instituto de Microelectrónica de Barcelona (IMB-CNM), University of Valencia and CSIC, Valencia, Spain
- 169 Department of Physics, University of British Columbia, Vancouver BC, Canada
- 170 Department of Physics and Astronomy, University of Victoria, Victoria BC, Canada
- 171 Department of Physics, University of Warwick, Coventry, United Kingdom
- 172 Waseda University, Tokyo, Japan
- 173 Department of Particle Physics, The Weizmann Institute of Science, Rehovot, Israel
- 174 Department of Physics, University of Wisconsin, Madison WI, United States of America
- 175 Fakultät für Physik und Astronomie, Julius-Maximilians-Universität, Würzburg, Germany
- 176 Fachbereich C Physik, Bergische Universität Wuppertal, Wuppertal, Germany
- 177 Department of Physics, Yale University, New Haven CT, United States of America
- 178 Yerevan Physics Institute, Yerevan, Armenia
- 179 Centre de Calcul de l'Institut National de Physique Nucléaire et de Physique des Particules (IN2P3), Villeurbanne, France
- ^a Also at Department of Physics, King's College London, London, United Kingdom
- ^b Also at Laboratório de Instrumentação e Física Experimental de Partículas - LIP, Lisboa, Portugal
- ^c Also at Faculdade de Ciências and CFNUL, Universidade de Lisboa, Lisboa, Portugal
- ^d Also at Particle Physics Department, Rutherford Appleton Laboratory, Didcot, United Kingdom
- ^e Also at TRIUMF, Vancouver BC, Canada
- ^f Also at Department of Physics, California State University, Fresno CA, United States of America
- ^g Also at Novosibirsk State University, Novosibirsk, Russia
- ^h Also at Department of Physics, University of Coimbra, Coimbra, Portugal
- ⁱ Also at Università di Napoli Parthenope, Napoli, Italy

- ^j Also at Institute of Particle Physics (IPP), Canada
- ^k Also at Department of Physics, Middle East Technical University, Ankara, Turkey
- ^l Also at Louisiana Tech University, Ruston LA, United States of America
- ^m Also at Dep Fisica and CEFITEC of Faculdade de Ciencias e Tecnologia, Universidade Nova de Lisboa, Caparica, Portugal
- ⁿ Also at Department of Physics and Astronomy, Michigan State University, East Lansing MI, United States of America
- ^o Also at Department of Financial and Management Engineering, University of the Aegean, Chios, Greece
- ^p Also at Department of Physics, University of Cape Town, Cape Town, South Africa
- ^q Also at Institute of Physics, Azerbaijan Academy of Sciences, Baku, Azerbaijan
- ^r Also at Institut für Experimentalphysik, Universität Hamburg, Hamburg, Germany
- ^s Also at Manhattan College, New York NY, United States of America
- ^t Also at CPPM, Aix-Marseille Université and CNRS/IN2P3, Marseille, France
- ^u Also at School of Physics and Engineering, Sun Yat-sen University, Guanzhou, China
- ^v Also at Academia Sinica Grid Computing, Institute of Physics, Academia Sinica, Taipei, Taiwan
- ^w Also at Laboratoire de Physique Nucléaire et de Hautes Energies, UPMC and Université Paris-Diderot and CNRS/IN2P3, Paris, France
- ^x Also at School of Physical Sciences, National Institute of Science Education and Research, Bhubaneswar, India
- ^y Also at Dipartimento di Fisica, Università La Sapienza, Roma, Italy
- ^z Also at DSM/IRFU (Institut de Recherches sur les Lois Fondamentales de l'Univers), CEA Saclay (Commissariat à l'Energie Atomique et aux Energies Alternatives), Gif-sur-Yvette, France
- ^{aa} Also at Moscow Institute of Physics and Technology State University, Dolgoprudny, Russia
- ^{ab} Also at section de Physique, Université de Genève, Geneva, Switzerland
- ^{ac} Also at Departamento de Fisica, Universidade de Minho, Braga, Portugal
- ^{ad} Also at Department of Physics, The University of Texas at Austin, Austin TX, United States of America
- ^{ae} Also at Department of Physics and Astronomy, University of South Carolina, Columbia SC, United States of America
- ^{af} Also at Institute for Particle and Nuclear Physics, Wigner Research Centre for Physics, Budapest, Hungary
- ^{ag} Also at DESY, Hamburg and Zeuthen, Germany
- ^{ah} Also at International School for Advanced Studies (SISSA), Trieste, Italy
- ^{ai} Also at Faculty of Physics, M.V.Lomonosov Moscow State University, Moscow, Russia
- ^{aj} Also at Nevis Laboratory, Columbia University, Irvington NY, United States of America
- ^{ak} Also at Physics Department, Brookhaven National Laboratory, Upton NY, United States of America
- ^{al} Also at Department of Physics, Oxford University, Oxford, United Kingdom
- ^{am} Also at Discipline of Physics, University of KwaZulu-Natal, Durban, South Africa
- * Deceased